Modelling Heat transfer coefficient in nanofluids in gravity based pipe flow

A

THESIS

Submitted in partial fulfillment of the requirement for the award of degree of

Master of Engineering

In

Thermal Engineering

Submitted by

KARANVEER SINGH MANGAT

(Roll No. 801283013)

UNDER THE GUIDANCE OF

DR. S.S. MALLICK

(ASSISTANT PROFESSOR)

Department of Mechanical Engineering

THAPAR UNIVERSITY, PATIALA – 147004

CERTIFICATION

I, Karanveer Singh Mangat, declare that this thesis report on modeling heat transfer coefficient in nanofluids in gravity based pipe flow, submitted towards fulfillment of the requirements for the award of master's degree in Thermal engineering in the Mechanical department, Thapar University, Patiala is wholly my own work. This document has not been submitted for any degree at any other institute.

Date: 2-08-2014
Place: Thapar

Karanveer Singh

Karanveer Singh Mangat
801283013
Thermal engineering
Thapar University, Patiala

This is to certify that the above statement made by the candidate is correct and true to the best of my knowledge.

Guide:
Dr. S.S. Mallick
Assistant Professor
Mechanical Engineering Department
Thapar University, Patiala

Countersigned by

Dr. Ajay Batish
Professor and Head
Mechanical Engineering Department
Thapar University, Patiala

Dr. S.K. Mohapatra
Dean
Academic Affairs
Thapar University, Patiala

ii

ACKNOWLEDGEMENT

No volume of words is enough to express my gratitude towards my guide**,** Dr. S.S. Mallick, Department of Mechanical Engineering, Thapar University, Patiala, who has been very concerned and has aided for all the material essential for the preparation of this report. He has helped me explore this vast topic in an organized manner and provided me with all the ideas on how to work towards a research-oriented venture.

Last but not least, I am forever grateful to my parents for their unconditional support and best wishes.

Karanveer Singh Mangat
801283013
Thermal engineering
Thapar University, Patiala

Contents page

Abstract

Heat transfer is one of the most important processes in many industrial. The inherently poor thermal performance of common fluids put a limitation and restricted in developing energy efficient heat transfer fluid. With a strong needed by industry in developing energy efficient, advance heat transfer fluid called nanofluid is introduced. Nanofluid is prepared by two step technique in this study by diluting Alumina CuO, and TiO_2 Nanoparticle with water at concentration of .01% The heat transfer coefficient was investigated experimentally in a flow in three tubes of diameters 15.875mm,12.7mm and 9.52mm respectively with Reynolds no. in range of 1000-4500. Initial experiments were conducted with pure water for experiment validation and accuracy. The experimental results, represented in Nusselt number (*Nu*) are compared to classical Gnielinski equation and Dittus-Boelter equation and observed that both equations are applicable in turbulent flow range for single phase fluid but some deviation 0f 5-10% was observed. The model developed from use of 3 different nanofluids at 0.01%volume fraction is dependent on ratio of particle diameter to pipe diameter and on the ratio of particle density to fluid density. So the derived model is dependent on different parameters than found in most of literature. It gives error of 5-15% when compared with other models dependent on different parameters. To eradicate this error further research can be done on to find other parameters that influence the convection heat transfer coefficient

Chapter 1

Introduction and objective

1.1 Inroduction

Nanofluids are a suspension of nanoparticles in a base fluid (e.g. water, ethylene glycol etc.). A nanoparticle can be defined as a quasi-zero dimensional object in which all characteristic linear dimensions are of the nano-size order of magnitude (Choi, 1995). .Nanofluids are very promising fluids especially in fields involving heat transfer due to their anomalously high thermal conductivity(10-25% higher than base fluids in volume fractions of 1-5 %)The thermal conductivity of a nanofluid containing some volume fraction of nanoparticles is found to be higher than the thermal conductivity of a fluid containing the same volume fraction of millimeter or micrometer sized particles (Eastman et. al. 2002).The problems occurring from the micrometer size particles are: rapid settlement, abrasion, fouling of components and clogging of flow passages (Kwak and Kim, 2005). These problems are significantly mitigated by use of nanoparticles in suspension. Their increased thermal conductivity is attributed to many factors like aggregation, Brownian motion etc .due to their property of enhancement of thermal conductivity.

Earlier small sized nanoparticles were difficult to synthesize and characterize, however modern day technology has helped in the synthesis of particles of nanometer size. The materials made of nanometer-sized particles fabricated on the atomic or molecular demonstrate either new or enhanced physical properties that are not exhibited by the material in bulk. These properties include the thermal, mechanical, optical, magnetic and electrical properties. This uniqueness in the properties has been attributed to the high surface area/volume ratio of the nanostructured materials. As a consequence of this, research and development in the field of nanophase materials has drawn considerable attention (Duncan and Rouveray, 1989)

There are many challenges strewn in the path of nanofluids being used commercially as an effective heat transfer medium. This is mainly due to three reasons. Firstly, the properties of nanofluids have been very difficult to understand and even more difficult to model. It is because there are a number of parameters that have to be studied associated with the nanoparticles and also the base fluid such as the particle size, temperatures, pressure, specific heat, thermal conductivity, viscosity and the interaction of the particles with the fluid medium. Secondly, it's a field that involves interdisciplinary knowledge (i.e knowledge of chemistry, physics, fluid mechanics etc) and hence relatively more difficult. (Foley et al 2006) Thirdly, even though nanofluids are expected to remain stable due to vigorous Brownian motion of the suspended nanoparticles (Hwang et al., 2006, Keblinski et al., 2002), this is not the case. The nanoparticles agglomerate and form clusters and this reduction in the stability is a hindrance not only because it may cause clogging and abrasion of channels but also because it leads to decrease in the thermal conductivity improvement (Hong et al., 2006). Contrary to this theory, however, is another theory according to which aggregation is a more likely cause for the enhancement of thermal conductivity of nanofluid (Gharagozloo and Goodson, 2010). Thus there is no agreement between the various research groups about the relation of particle agglomeration, Brownian motion in nanofluids and other phenomenon like laminar layer, turbulent flow etc and their effect on convection heat transfer coefficient. This is the reason of undertaking this effort to derive a model experimentally that shows dependence of heat transfer coefficient on parameters like ratio of particle diameter to pipe diameter, ratio of particle density to nanofluid density

1.2 Objectives:

Specific objectives include:

1) To study the heat transfer variations arising from use of different nanofluids in different diameters of pipes used.

2) To develop a model for Nusselt number that is dependent on ratio of particle diameter to pipe diameter and on ratio of particle density to nanofluid density.

3 To validate that model with unused experimental readings to confirm its applicability.

Chapter 2:

Literature Review

This chapter consists of a detailed study of nanofluids, the various materials that make up nanoparticles and the base fluids that are used, the methods of synthesis of nanoparticles and nanofluids, applications of nanofluids. the measurement techniques that are used to measure various parameters that are used to study the nanofluids such as stability and thermal conductivity, characterization techniques and a review of the experimental work that has been done by other researchers. While choosing nanoparticles and base fluids, the following points must be considered:

(i) The system must be electrically non-conductive

(ii) The system must have high thermal and heat transfer properties.

(iii) The system must have high density and specific heat so that lesser volume of

coolant is required to be circulated to provide cooling.

(iv) The system should have low viscosity so that lesser pumping power is exerted.

(v) The system should be non corrosive

(vi) The nanofluid system should be stable.

(vii) No flammability and toxicity

2.1Synthesis of nanofluid

Physical process and chemical process have been used to prepare nanoparticles. Physical process includes inert gas condensation. In the gas phase condensation process under inert and cool conditions source material is evaporated and quickly condensed from vapor into nanometer size particles or loosely agglomerated clusters under reduced pressure atmosphere (Eastman et al. 2000) .For water soluble materials chemistry-based solution-spray conversion process is used. Conversion to aerosol of solution is done then and for drying a spray drying system used. Quick vaporization of solvent and quick precipitation of solute retains the composition similar to starting solution. The parent chemical powder is kept in a fluidised-bed reactor to evenly pyrolyze mixture to drive out volatile part and make porous powders of uniform fine homogeneous structure.

If nanoparticles are made up of any of these methods there is some form of agglomeration of smaller particles. Production of non-agglomerated nanoparticles requires condensing nanophase powders present in vapor phase directly to flowing low-vapor pressure fluids called the VEROS (Vacuum Evaporation onto a Running Oil Substrate) technique and this approach is developed by (Akoh et al. 1978). VEROS has been essentially avoided by the nanocrystalline-materials community because of difficulties in subsequently separating the particles from the fluids to make bulk materials or dry powders. Modification of the VEROS technique is developed in Germany developed that is a direct evaporation system based on the modification in VEROS technique. Stable suspension of nanoparticles in conventional base fluids (water, oil and ethylene glycol) i.e. nanofluids are prepared by two techniques: the single step technique and the two step technique (Das et al., 2007 and Chon, 1999).

The single step method simultaneously prepares and disperses nanoparticles directly into conventional base fluids. The two step method first prepares nanoparticles using physical or chemical process to prepare nanoparticles and disperses these nanoparticles into conventional base fluids (Das et al., 2007 and Choi, 1999). Ultrasonicator Das et al., 2007) and magnetic stirrer (Sundar et al., 2007) are used to prepare nanofluids by two step technique, commonly bath or prob type ultrasonicator is used to prepare nanofluids (Das et al., 2007).

A submerged arc nanoparticle synthesis system (SANSS) was developed to prepare CuO nanoparticles dispersed uniformly in a dielectric liquid (deionized water). The method successfully produced a stable nanofluid in principle; a pure copper rod is submerged in a dielectric liquid in a vacuum chamber. A suitable electric power source is used to produce an arc between 6000 - 12000 °C which melts and vaporizes the metal rod in the region where the arc is generated. At the same time, the deionized water is also vaporized by the arc (Zhu et al. 2004). The vaporized metal undergoes nucleation, growth and condensation resulting in nanoparticles dispersed in deionized water. Nanofluids containing CuO particles of size 49.1 ± 38.9 nm were obtained.

Some methods to produce nanoparticles chemically are :

(i) Transition metal salt reduction

(ii) Thermal decomposition and photochemical methods

(iii) Ligand reduction and displacement from organometallics

(iv) Metal vapor synthesis, and

(v) Electrochemical synthesis

(vi)Transition-metal nanoclusters are only kinetically stable because the formation of the bulk metal is its thermodynamic minimum.

(Bonnemann et al 2003)developed a method for the production of very small (< 2 nm) and stable nanoparticles via chemical reduction pathways, which might be suitable for application in nanofluid synthesis. Organ aluminum compounds have been used for the "reductive stabilization" of mono and bi-metallic nanoparticles. Triorganoaluminum compounds were employed as both the reducing agent and colloid stabilizer, which lead to the formation of an organo-metallic colloidal protecting shell around the particles This "modification" of the Al-organic protecting shell leaves the particle size stable. Highly conductive Silver nanoparticles are one of the most widely studied nanomaterials because they exhibit unusual optical, electronic and chemical properties, which depend on their size, and shape .Due to its high thermally conductivity, silver's cooling applications would be interesting.

Besides silver nanoparticles, (Xuan et al. 2004**)** have used commercially obtained Cu nanoparticles to prepare nanofluids in both water and transformer oil by sonication in the presence of stabilizers. Similarly, (Kim et al. 2006) prepared nanofluids consisting of commercially obtained CuO nanoparticles in ethylene glycol by sonication without stabilizers. The optimum duration of sonication was found to be 9 hours and the average nanoparticle size was 60 nm. The two-step process is commonly used for the synthesis of carbon nanotube based nanofluids. Single-wall carbon nanotubes (SWCNTs) and Multi-walled carbon nanotubes (MWCNTs) are cylindrical allotropes of carbon. SWCNTs consist of a single cylinder of

graphene, while MWCNTs contain multiple graphene cylinders nesting within each other .The carbon nanotubes are usually produced by a pyrolysis method and then suspended in a base fluid with or without the use of a surfactant. Some authors suggested that the two-step process works well only for nanofluids containing oxide nanoparticles dispersed in de-ionized water as opposed to those containing heavier metallic nanoparticles. Since nanopowders can be obtained commercially in large quantities, some economic advantage exists in using two-step synthesis methods that rely on the use of such powders.

The major problem with two step method is aggregation of nanoparticles. It has been shown that particles strongly aggregated before dispersion are still in an aggregated state after dispersion in ethylene glycol and 9 hours of sonication (Kwak and Kim, 2005). Ultrasonic equipment is used to intensively disperse the particles and reduce agglomeration. Apart from that the use of other techniques such as control of pH or addition of surface active agents is made to avoid agglomeration and sedimentation.

2.2Cooling applications of nanofluids:

Cooling applications form a bulk of scope for use of nanofluids. The main requisite for an effective cooling effect is high convection heat transfer coefficient. This coefficient is dependent on parameters like conductivity, specific heat, density, dimensions and shape of flow bodies. Some examples of cooling applications are:

Cooling of Microchips

A principal limitation on developing smaller microchips is the rapid heat dissipation. However, nanofluids can be used for liquid cooling of computer processors due to their high thermal

conductivity. It is predicted that the next generation of computer chips will produce localized heat flux over 10 MW/ m^2 with the total power exceeding 300 W. In combination with thin film evaporation, the nanofluid oscillating heat pipe (OHP) cooling system will be able to remove heat fluxes over 10 MW/m^2 and serve as the next generation cooling device that will be able to handle the heat dissipation coming from new technology.

Even though nanofluids and OHPs are not new discoveries, combining their unique features allows for the nanoparticles to be completely suspended in the base liquid increasing their heat transport capability. Since nanofluids have a strong temperature-dependent thermal conductivity

They show a nonlinear relationship between thermal conductivity and concentration, they are high performance conductors with an increased CHF. The OHP takes intense heat from a high-power device and converts it into kinetic energy of fluids while not allowing the liquid and vapor phases to interfere with each other since they flow in the same direction.

Nanofluid in Fuel

The aluminum nanoparticles, produced using a plasma arc system, are covered with thin layers of aluminum oxide, owing to the high oxidation activity of pure aluminum, thus creating a larger contact surface area with water and allowing for increased decomposition of hydrogen from water during the combustion process. During this combustion process, the alumina acts as a catalyst and the aluminum nanoparticles then serve to decompose the water to yield more hydrogen. It was shown that the combustion of diesel fuel mixed with aqueous aluminum

nanofluid increased the total combustion heat while decreasing the concentration of smoke and nitrous oxide in the exhaust emission from the diesel engine (Kao et al 2007)

Smart Fluids

In this new age of energy awareness, our lack of abundant sources of clean energy and the widespread dissemination of battery operated devices, such as cell-phones and laptops, have accented the necessity for a smart technological handling of energetic resources. Nanofluids have been demonstrated to be able to handle this role in some instances as a smart fluid. In a recent paper published in the March 2009 issue of Physical Review Letters, (Donzelli et al 2009). showed that a particular class of nanofluids can be used as a smart material working as a heat valve to control the flow of heat. The nanofluid can be readily configured either in a "low" state, where it conducts heat poorly, or in a "high" state, where the dissipation is more efficient. To leap the chasm to heating and cooling technologies, the researchers will have to show more evidence of a stable operating system that responds to a larger range of heat flux inputs.

Industrial Cooling Applications

Routbort et al. [2009] started a project in 2008 that employed nanofluids for industrial cooling that could result in great energy savings and resulting emissions reductions. For U.S. industry, the replacement of cooling and heating water with nanofluids has the potential to conserve 1 trillion Btu of energy. For the U.S. electric power industry, using nanofluids in closed-loop

cooling cycles could save about 10–30 trillion Btu per year (equivalent to the annual energy consumption of about 50,000–150,000 households). The associated emissions reductions would be approximately 5.6 million metric tons of carbon dioxide; 8,600 metric tons of nitrogen oxides; and 21,000 metric tons of sulfur dioxide.

Nuclear Reactors

Kim et al. (2007,207) at the Nuclear Science and Engineering Department of the Massachusetts Institute of Technology (MIT), performed a study to assess the feasibility of nanofluids in nuclear applications by improving the performance of any water-cooled nuclear system that is heat removal limited. Possible applications include pressurized water reactor (PWR) primary coolant, standby safety systems, accelerator targets, plasma divertors, and so forth, In a pressurized water reactor (PWR) nuclear power plant system, the limiting process in the generation of steam is critical heat flux (CHF) between the fuels rods and the water—when vapor bubbles that end up covering the surface of the fuel rods conduct very little heat as opposed to liquid water. Using nanofluids instead of water, the fuel rods become coated with nanoparticles such as alumina, which actually push newly formed bubbles away, preventing the formation of a layer of vapor around the rod and subsequently increasing the CHF significantly. After testing in MIT's Nuclear Research Reactor, their preliminary experiments have shown promising success where it is seen that PWR is significantly more productive. The use of nanofluids as a coolant could also be used in emergency cooling systems, where they could cool down overheat surfaces more quickly leading to an improvement in power plant safety

Extraction of Geothermal Power and Other Energy Sources

The world's total geothermal energy resources were calculated to be over 13000 ZJ in a report from MIT. Currently only 200 ZJ would be extractable, however, with technological improvements, over 2,000 ZJ could be extracted and supply the world's energy needs for several millennia. When extracting energy from the earth's crust that varies in length between 5 to 10 km and temperature between 500°C and 1000°C, nanofluids can be employed to cool the pipes exposed to such high temperatures. When drilling, nanofluids can serve in cooling the machinery and equipment working in high friction and high temperature environment. As a "fluid superconductor," nanofluids could be used as a working fluid to extract energy from the earth core and processed in a PWR power plant system producing large amounts of work energy.

Tran et al.(2007), funded by the United States Department of Energy (USDOE), performed research targeted at developing a new class of highly specialized drilling fluids that may have superior performance in high temperature drilling. This research is applicable to high pressure high temperature drilling, which may be pivotal in opening up large quantities of previously unrecoverable domestic fuel resources. Commercialization would be the bottleneck of progress in this sub-area.

Nanofluid Coolant in automobiles:

In looking for ways to improve the aerodynamic designs of vehicles, and subsequently the fuel economy, manufacturers must reduce the amount of energy needed to overcome wind resistance on the road. At high speeds, approximately 65% of the total energy output from a truck is expended in overcoming the aerodynamic drag. This fact is partly due to the large radiator in front of the engine positioned to maximize the cooling effect of oncoming air. The use of

nanofluids as coolants would allow for smaller size and better positioning of the radiators. Owing to the fact that there would be less fluid due to the higher efficiency, coolant pumps could be shrunk and truck engines could be operated at higher temperatures allowing for more horsepower while still meeting stringent emission standards.

Argonne researchers,(Singh et al. 2006), have determined that the use of high-thermal conductive nanofluids in radiators can lead to a reduction in the frontal area of the radiator by up to 10%. This reduction in aerodynamic drag can lead to a fuel savings of up to 5%. The application of nanofluid also contributed to a reduction of friction and wear, reducing parasitic losses, operation of components such as pumps and compressors, and subsequently leading to more than 6% fuel savings. It is conceivable that greater improvement of savings could be obtained in the future.

In order to determine whether nanofluids degrade radiator material, they have built and calibrated an apparatus that can emulate the coolant flow in a radiator and are currently testing and measuring material loss of typical radiator materials by various nanofluids. Erosion of radiator material is determined by weight loss-measurements as a function of fluid velocity and impact angle.

In their tests, they observed no erosion using nanofluids made from base fluids ethylene and tri-cloroethylene glycols with velocities as high as 9 m/s and at impact angles. There was erosion observed with copper nanofluid at a velocity of 9.6 m/s and impact angle of 30°-90°. The corresponding recession rate was calculated to be 0.065 mils/yr of vehicle operation

2.3 Characterization of nanofluids:

Characterization of nanoparticles once they have been synthesized allows looking into the structure of the nanoparticles and forms an important part of research. Reliable Methods for characterizing nanofluids are critical to a correct understanding of their novel properties. The particle size is a very important factor that needs to be taken into consideration in the study of nanofluids for the following reasons. Firstly, particle size matters in making nanofluid stable. Dense nanoparticles can be suspended in liquids because the particles have an extremely high ratio of surface area to volume so that the interaction of the particle surface with the liquid is strong enough to overcome differences in density (i.e. the gravity effect is negligible). Secondly, size matters in making nanofluids with novel properties. Thirdly, particle size matters in making nanofluids useful in some applications. Since the size of nanoparticles is similar to that of bio-molecules, nanofluids can be used in bio-medical applications such as drug delivery and nanofluids based control of biological functions (Choi, 2009). Following is a description of the various techniques that are used for the nanofluid characterization.

(i) X-ray diffraction analysis (XRD): X-ray diffraction is an important technique to understand the properties of synthesis materials. X-ray diffraction is a fast technique and for XRD small amount of sample is required which is non destructive. With the help of data base of known structure XRD is used for the phase identification and XRD is also used to determine crystal structure of unknown materials, strain, crystal size, orientation of single crystal or polycrystalline materials (Cullity and Stock 2001) Suryanarayana and Norton 1998 and Waseda et al., 2001).

(Cullity and Stock 2001), and (Waseda et al., 2001)explained the principle of operation of X-ray diffraction analysis, when X-rays are directed on the sample, electrons present in the material scatter the X-rays. Scattering results in maxima and minima of different intensity, if the material

is crystalline. Bragg's law provides the conditions that must be satisfy for the reflected X-ray waves to be in phase with each other (constructive interference).

If conditions of Bragg's law are not satisfied, destructive interference reduces the reflected intensity to zero. Bragg's law is $\lambda = 2D\sin\theta$. Here λ is the X-ray wavelength, m' is an integer, θ is the diffraction angle and D is the distance between crystal lattice planes. For each lattice spacing D, Bragg's law predicts a maximum at diffraction angle θ. An X-ray diffraction pattern is obtained when the intensity of detected X-rays is plotted as a function of diffraction angle θ. To identify the phase of tested sample XRD Patten is matched with the pure substance. The plot obtained from XRD analysis shows the characteristic of the sample material.

(ii) Scanning Electron Microscopy (SEM): Scanning Electron Microscopy is a powerful method to investigate the surface structures of mollicutes. SEM is standardized method for imaging and the measuring the dimensions of nanometer and micrometer size particles because of high imaging speed and high resolution of SEM (Buhr et al., 2009). This technique provides a large depth of field. SEM has relatively wide range of magnification which allows the investigator to easily focus in an area of interest on a specimen; an investigator may easily interpret SEM images (Stadtlander, 2007). Gabriel (1985) discussed about the operating conduction and operation of SEM: the basic operating condition for SEM involves high vacuum with minimum contagion, properly aligned column and saturated filament to its effective operating temperature. After setting the basic operating condition, for a given specimen the optimal imaging conditions are controlled by spot size, accelerating voltage and focus. Prepared specimen should be clean and conductive.

Sometimes the filament is not heated until high vacuum is maintained. The alignment of column is evaluated, after filament has been saturated. Alignment of electron gun is evaluated in reduced rapid or TV scan rate. In both the scanning mode, manipulate the gun X and Y electronic controls until uniform bright and centered image in CRT is obtained. Focus the image at about 1000X in rapid or TV mode. Select a view field where symmetrical object is able to be seen. If the image is not expanding symmetrically from its centre, correct its asymmetry by manipulating the stigmators.

If the stigmator is not able to correct the asymmetry, the final aperture is off axis. Then again correct the stigmators by moving the aperture X and Y. After correcting the asymmetry, set the magnification and evaluate the specimen. A series of images from low to high magnification is obtained to examine the specimen. After finishing the examination, filament should be cooled for minimum 3 minutes before chamber is subjected to atmospheric pressure.

(iii) Transmission Electron Microscopy (TEM): Transmission electron microscopy (TEM) is also a standardized method for imaging and measurements of dimension of nano and micro size structures due to their high imaging speed and high resolution (Buhr et al., 2009). The advantage of TEM over SEM is that the specimen's cellular structures can be viewed at extremely high magnifications (Stadtlander, 2007).

Cullity and Stock (2001) explained the operation of TEM. TEM is a complex assembly of magnetic lenses, electron gun, a sample holder, several apertures and image viewing/ recording systems. Magnetic lenses are set into illuminating systems between sample and electron gun and those of imaging system after sample.

There are three lenses in the imaging system and two condenser lenses in the illumination system. The traditional TEM mode adjusts condense lenses to illuminate the sample with approximately parallel beam. Beam covers sample area of several micrometer diameters at magnification lies between 20,000X and 100,000X. To control beam position or angle pre-specimen scanning or deflection coils are often used.

In TEM to view the diffraction pattern, the intermediate lens is set to focus on the back focal plane of objective lens. In the case of viewing the image the intermediate lens is adjusted so that its object plane is plane of image of the objective lenses. If all the transmitted beams and diffraction beams were directed to combine in the first intermediate image plane, resultant images would be of little contrast.

2.4 Measurement of thermal conductivity of nanofluids

Two types of methods are available for measuring the thermal conductivity of nanofluids: steady state methods and transient methods. Transient methods are best for accurate measurement of thermal conductivity of fluids/nanofluids. Steady state methods are less accurate than transient methods because in steady state methods heat lose cannot be quantified and may provide considerable inaccuracy and natural convection may also set in, which provides apparently higher value of thermal conductivity (Das et al., 2007). Most popularly used methods of transient and steady state method in literature are discussed in detail:

2.4.1Transient hot-wire method

Principle of measurement: Transient hot wire method is most accurate, fast and widely used method for the measurement of thermal conductivity of. In this method a thin wire of metal is used as both a temperature sensor and a line heat source. Liquid whose thermal conductivity is measured surrounds the thin metallic wire. Thin metallic wire is heated by passing current through it. Now, if the thermal conductivity of the surrounding liquid is higher than there will be lower rise in the temperature of wire. Experiment is preformed for short duration of time (2 to 8 seconds), so that natural convection cannot set. This is the principle on which this method works.

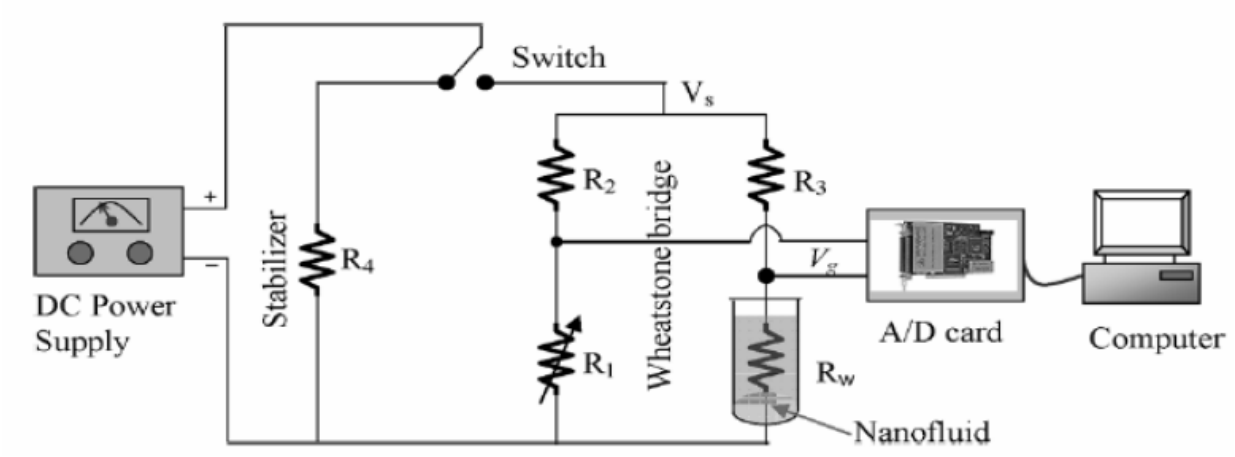

Figure2.4.1.1: Schematic of transient hot wire experimental setup by(Murshed et al., 2005).

To explain the working of transient hot wire apparatus specifications of (Murshed et al. 2005) are considered i.e. platinum wire of 76 micrometer diameter and 215 mm length and container is of 80 ml and diameter of container is 20 mm. A schematic of the transient hot-wire apparatus used by Murshed et al. (2005) is given in Figure 1. As shown in Figure 1 main experimental cell is a

part of the Wheatstone bridge circuit. Thin platinum wire is used as an arm of the Wheatstone bridge circuit.

Platinum wire has been used because of higher electrical resistivity and order of higher magnitude than that of any other material and Platinum wire has temperature coefficient of resistance of 0.0039092°C which is higher than any other material (Das et al., 2007; Murshed et al., 2005). Wire should be of smaller diameter to act as a line heat source. The Wheatstone bridge circuit was balanced by adjusting the adjustable circuit resistance and ground resistance of A/D (analog to digital) converter input panel. Circuit was considered as balance circuit when there is no voltage change observed in A/D converter.

When a uniform voltage is supplied to the circuit, the temperature and electric resistance of the wire rises and the output voltage is measured by an A/D convertor. The obtained data of temperature rise is linear against logarithmic time interval. The thermal conductivity is calculated from the slope of the rise in the wire's temperature against logarithmic time interval by the equation 1 (Das et al., 2007).

$$K_{nf} = [Q*\{\ln(i_1/i_2)\}]/\{4\pi(T_2-T_1)\} \quad (1)$$

2.4.2 Transient short-hot-wire (SHW) method

Principle of measurement: Transient SHW technique is used to measure the thermal conductivity and thermal diffusivity of nanofluids simultaneously (Zhang et al., 2000). Zhang et al. (2000) explained the principle of operation of transient SHW technique in detail. Zhang et al.(2000) explained that (SHW) technique was developed from the conventional transient hot wire method. This technique is also based on the two-dimensional transient heat conduction numerical solution for a short wire of the same length-to-diameter ratio and boundary conditions

as those used in the actual measurements. The thermal conductivity of nanofluids in transient SHW technique is calculated by equation 2 :

$$K_{nf} = \frac{VIE}{2\pi he} \qquad (2)$$

Coefficient E is calculated by the least-squares method for a relevant range of Fourier number corresponding to the periods of measurement. Coefficient e is also determined by the least squares which is supported by a ceramic circular plate res method for time range before the onset of natural convection. To explain the working of this method specification of Zhang et al. (2000) are considered. Figure 2 shows the schematic of transient SHW cell. The SHW probe is set on the Teflon cap of the cell. A short platinum wire of 9.2 mm length and 97 micrometer diameter.

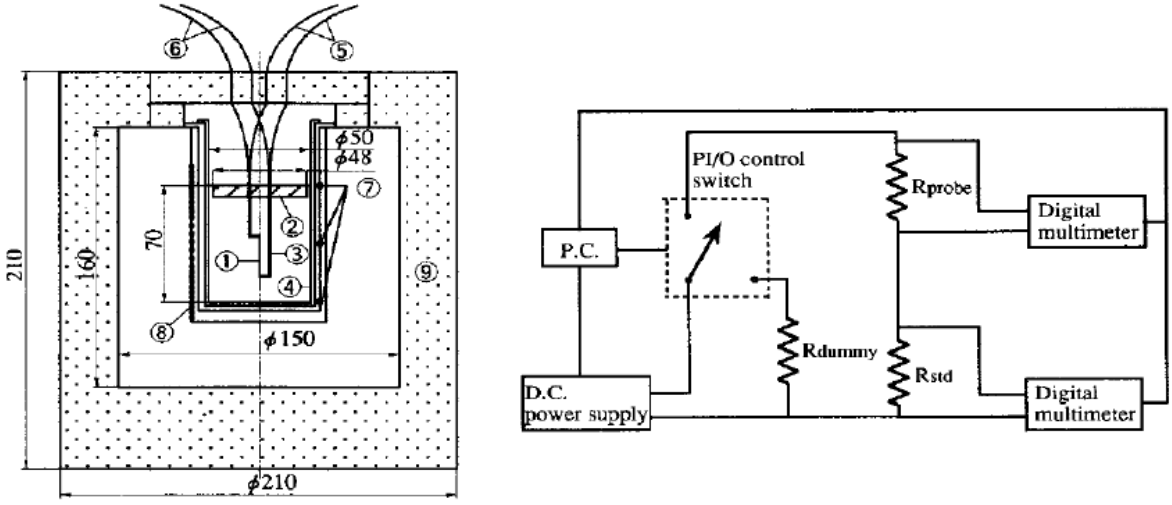

Figure 2.4.2.1: Schematic of experimental setup and measurement system by Zhang et al., 2000

(1) A short platinum wire of 9.2 mm length and 97 micrometer diameter is welded at the both ends to 1.5 mm diameter platinum lead wire

(2) And joined with voltage

(3) Which is supported by a ceramic circular plate

(4) of 50 mm diameter and 120 cm3 volume is heated with an electric furnace

5) And current

(6) Platinum lead wires of 0.5 mm diameter. A pure gold crucible

(8) Which is outside covered with a thermal insulator.

(9)The temperatures at the outside wall of crucible are measured with thermocouples

(7) To give a feedback signal for the temperature controller.

The measurements have to carry at atmospheric pressure and different temperature levels. Platinum wire is welded to the platinum lead terminals. Alumina is used as a coated material which is 99.99% pure. The sputtering time is 6.4 h for Al_2O_3 film thickness of 2 μm. Sputtering apparatus provide a thin uniform film on the cylindrical wire. The measuring system of SHW technique is also shown in Figure 2. Measuring system is composed of a d/c power supply current and voltage measuring system, digital multimeter, power input/output (PI/O) controller and personal computer. A maximum constant current of 1 A with 1.5 mA resolution cab be generated by power supply. When the liquid temperature becomes uniform and constant, a small current of 15 mA, is supplied to the probe for 3 s for the measurement of initial temperature of liquid. The switch is turned on to the dummy circuit. Dummy circuit is having the same resistance as the main circuit including the probe. A heating current of 0.3 to 0.5 A is supplied. When the current becomes stable (After 1 second,), the switch is closed to the main circuit to

begin heating the hot wire. In this process, the voltage and current are measured 20 times per sec. All the measurements are carried out automatically using a personal computer.

2.4.3 Temperature oscillation method

Principle of measurement: The principle of thermal conductivity measurement is based on the propagation of temperature oscillation inside a cylindrical liquid volume. The measurement of thermal conductivity is based on energy equation for conduction which is given by equation 3:

$$\nabla^2 T = \frac{1}{\alpha} * \frac{\partial T}{\partial t} \qquad (3)$$

The assumptions for the equation 3 in this case are the test fluid is isentropic and thermo physical properties are constant and uniform with time throughout the entire specimen volume. Das et al. (2003) explained the experimental set up and procedure for the measurement of thermal conductivity. Experimental set up by Das et al. (2003) is shown in Figure 3.

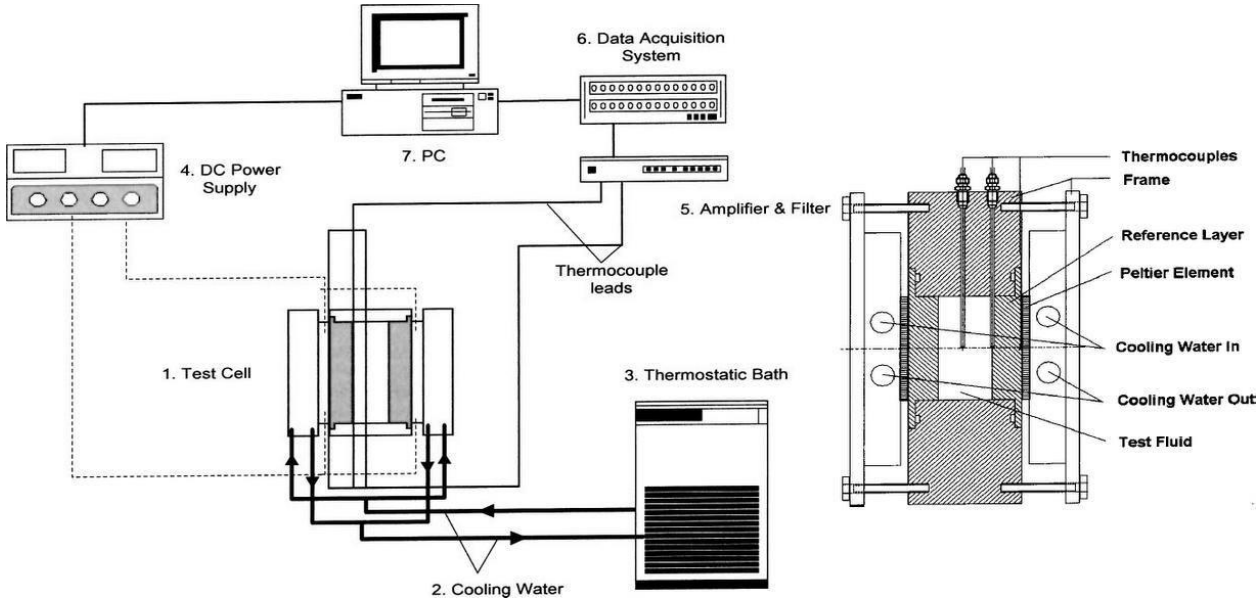

Figure 2.4.3.1 : Schematic of experimental setup and test cell by Das et al. 2003

Das et al. (2003) described that this technique consist of a specially fabricated test cell (1) which is cooled by cooling water (2) at both of the ends. Cooling water is coming from a thermostatic bath (3). Electrical connection provides DC power which is obtained through a converter (4). The temperatures are measured in the test section with the help of number of thermocouples and the responses are amplified with amplifier (5). Amplifier (5) is followed by a filter which is fed to the data acquisition system (6). The data logger in data acquisition system is, in turn connected to a computer (7). Temperature of the fluid is controlled by proper adjustment of the cooling water coming from the thermostatic bath. For higher temperatures, it is sometimes necessary to increase the input voltage to obtain the required temperature level which is then tuned to the required temperature by adjusting or maintain the cooling water temperature. The test section is also shown in Figure 3 which is a flat cylindrical cell. The frame of the cell is made of Polyoxymethylene, which acts as the first layer of insulation. The frame consists of a main part with 40 mm hole. Hole act as cavity to hold the test fluid. Frame also consist two end plates which sandwiches the Peltier element and water cooler at both ends. The hole is closed from both sides by disk type reference material of 15 mm thickness and 40 mm diameter. The space formed for the test fluid is 8 mm thickness and 40 mm diameter. The fluid is filled through a small hole in the cell body. The temperatures are measured at three locations—at the interface of the reference layer and the Peltier element, the central axial plane of the test fluid and at the interface of the test fluid and the reference layer. For this purpose, Ni-CrNi thermocouples of 0.1 mm in diameter were used at the interfaces and 0.5 mm in diameter at the central plane, for stability consideration. The thermocouples are put in small groove at the interfaces and welded at the tip, whereas the thermocouple at center is hanging from the wall.

The entire cell is insulated. The temperature of the reference material is periodically oscillated by two Peltier elements (40 mm×40 mm square) from two ends. For example an oscillated temperature recorded at the locations after reaching steady oscillation. It can be observed that the amplitude of the temperature oscillation produced by Peltier element gets attenuated and its phase shifts as it crossed the reference material. It is further shifted and attenuated as it reaches the center of the test fluid. Thermal diffusivity of the fluid can be calculated very accurately by considering amplitude attenuating of thermal oscillation from the boundary fluid to the center of the fluid.

For direct thermal conductivity measurement one has to consider the attenuation at the reference material. Since the reference material has been worked upon and inhomogenity and microcracks of material brings out uncertainty in its value of thermal conductivity, so the direct evaluation of thermal conductivity of fluid is not very accurate. Hence the value of thermal diffusivity for the nanofluid is evaluated from experiment. Density can be measured and specific heat can be calculated by equation 4:

$$C_{nf} = \left(\frac{m_p\, c_p + m_f c_f}{m_p + m_f}\right) \tag{4}$$

Finally the thermal conductivity is calculated by equation 5:

$$K_{nf} = (\alpha \rho c)_{nf} \tag{5}$$

2.5 Literature review of some related papers:

Mallick et al (2013) investigated and modeled thermal conductivity for alumina–water nanofluids, Evaluating seven existing theoretical models and empirical models for thermal conductivity of nanofluids for their accuracy. They did so by comparing the predicted versus experimental data for a wide range of test conditions. They found existing models to vary in inaccuracy (over/under-predictions) in the range of 2.34–58% .They undertook the study of Gleninski model (2009) given by:

$$\mathrm{Nu}=\frac{hD}{K}=\left(\frac{f/2\left(\mathrm{Re}-10^{3}\right)\mathrm{Pr}}{1+12.7(f/2)^{0.5}(Pr^{.66}-1)}\right)\left(1+\frac{D^{.66}}{L^{.66}}\right) \quad (6)$$

Its valid for 2300<Re<5000.

Here f=fanning friction factor given by

$$F=.25(\ln Re-1.64)^{-2}$$

This effort helped in representing the effects of micro-convection, localized turbulence and the ratio of heat transfer by diffusion to conduction for particle and fluids on the thermal conductivity of nanofluids. The Evaluation of new developed model was made by comparing the predicted results with experimental data; it revealed that the new model was within 5% accuracy for a wide range of data. Validation of this model has been done in this work of thesis also.

Wongwises et al (2008) studied Effect of thermo physical properties models on the predicting of the convective heat transfer coefficient for low concentration nanofluid. They asserted that in order to study the heat transfer behavior of the nanofluids, precise values of thermal and physical properties such as specific heat, viscosity and thermal conductivity of the nanofluids are required. There are a few well-known correlations for predicting the thermal and physical properties of nanofluids which are often cited by researchers to calculate the convective heat transfer behaviors of the nanofluids. Each researcher has used different models of the thermo physical properties in their works.

They summarized the various models for predicting the thermo physical properties of nanofluids which have been commonly cited by a number of researchers and use them to calculate the experimental convective heat transfer coefficient of the nanofluid flowing in a double-tube counter flow heat exchanger. The effects of these models on the predicted value of the convective heat transfer of nanofluid with low nanoparticle concentration were discussed in detail. The effects of the thermo physical properties model on the predicted values of the convective heat transfer coefficient of TiO_2–water nanofluid flowing in a horizontal double-tube counter flow heat exchanger under turbulent flow conditions were experimentally investigated. TiO_2 nanoparticles with 0.2 vol. % dispersed in water were used in the their study. The different models of the thermo physical properties of nanofluid gave different results. In the case of very low level of concentration, the various thermo physical models have no significant effect on the predicted values of the heat transfer coefficient.

Sundar et al (2009) conducted experiments to evaluate heat transfer coefficient and friction factor for flow in a tube. Experiments with twisted tape inserts in the transition range of flow with Al_2O_3 nanofluid were conducted. Their results showed considerable enhancement of

convective heat transfer with Al_2O_3 nanofluids compared to flow with water. They observed that the equation of (Gleninski et al 2009) applicable in transitional flow range for single-phase fluids showed considerable deviation when compared with values obtained with nanofluid. The heat transfer coefficient of nanofluid flowing in a tube with 0.1% volume concentration is 23.7% higher when compared with water at number of 9000. Heat transfer coefficient and pressure drop with nanofluid was experimentally determined with tapes of different twist ratios and found to deviate with values obtained from equations developed for single-phase flow. A regression equation was developed by them to estimate the Nusselt number valid for both water and nanofluid flowing in the transition flow Reynolds number range in circular plain tube and with tape inserts it is given by:

$$Nu=3.138*10^{-3}*Re*Pr^{.6}(1+H/D)^{.03}*(1+\varphi)^{1.22} \qquad (7)$$

The maximum friction factor with twisted tape at 0.1% nanofluid volume concentration is 1.21 times that of water flowing in a plain tube. They observed further heat transfer enhancement with twisted tape insert with H/D=5 inside a circular tube. Heat transfer rates with tape insert are obtained with nanofluid of 0.1% volume concentration, 36.96% at Reynolds number 3000 and 44.71% at Reynolds number 9000, compared to flow of nanofluid in a plain tube.

Pak and Cho (1998) investigated experimentally the turbulent friction and heat transfer behaviors of dispersed fluids (i.e., ultrafine metallic oxide particles suspended in water) in a circular pipe. Two different metallic oxide particles, alumina (Al_2O_3) and titanium dioxide (TiO_2) with mean diameters of 13 and 27 nm, respectively, were used as suspended particles. In their flow loop, the hydrodynamic entry section and the heat transfer section was made using a seamless, stainless steel tube, of which the inside diameter and the total length were 1.066 crn and 480 crn,

respectively. The hydrodynamic entry section was long enough (i.e., x/D = 157) to accomplish fully developed flow at the entrance of the heat transfer test section. They observed that the Nusselt number for the dispersed fluids increased with increasing volume concentration as well as Reynolds number. But at constant average velocity, the convective heat transfer coefficient of the dispersed fluid was 12% smaller than that of pure water. They proposed a new correlation for the Nusselt number under their experimental ranges of volume concentration (0-3%), the Reynolds number (104 - 105), and the Prandtl number (6.54 - 12.33) for the dispersed fluids □-Al2O3 and TiO2 particles as given by:

$$\mathbf{Nu=0.021Re^{0.8}\,Pr^{0.5}} \qquad (8)$$

Rao et al (2014) analyzed experimentally for heat transfer coefficient and friction factor of TiO_2 nanofluid flowing in a double pipe heat exchanger with and without helical coil inserts are studied experimentally. The experiments are conducted in the range of Reynolds number from 4000 to 15,000 and in the volume concentration range from 0.0004% to 0.02%. The base fluid is prepared by considering 40% of ethylene glycol and 60% of distilled water. The heat transfer coefficient and friction factor get enhanced by 10.73% and 8.73% for 0.02% volume concentration of nanofluid when compared to base fluid flowing in a tube. Heat transfer coefficient and friction factor further get enhanced by 13.85% and 10.69% respectively for 0.02% nanofluid when compared to base fluid flowing in a tube with helical coil insert of P/d = 2.5. They concluded that use of helical coil inserts is advantageous to enhance heat transfer on one hand and on the other hand it introduces undesirable pressure drop in the circuit. Much better performance in terms of heat transfer was observed with TiO_2 nanofluid over the conventional base fluid. The measured values of heat transfer coefficient and friction factor were compared with the published literature. Based on the experimental data, generalized correlations are

proposed for Nusselt number and friction factor. The results are presented in graphical and tabular form. Uncertainty analysis was also carried out and the experimental error was in the range of ±10%.

Sharma et al (2014) studied experimentally the comparison of convective heat transfer coefficient and friction factor of TiO_2 nanofluid flow in a tube with twisted tape inserts Their study reports a further enhancement in heat transfer coefficients in combination with structural modifications of flow systems namely, the addition of tape inserts. Experiments are undertaken to determine heat transfer coefficients and friction factor of TiO_2-water nanofluid up to 3.0% volume concentration at an average temperature of 30°C. The investigations are undertaken in the Reynolds number range of 8000-30000 for flow in tubes and with tapes of different twist ratios. They used following model and validated it:

$$Nu=\frac{hD}{K}=.27Re^{.693}Pr^{-0.3}*(1+D/H)^{1.3} \quad (9)$$

A significant enhancement of 23.2% in the heat transfer coefficients is observed at 1.0% concentration for flow in a tube. With the use of twisted tapes, the heat transfer coefficient increased with decrease in twist ratio for water and nanofluid. The heat transfer coefficient and friction factor are respectively 81.1% and 1.5 times greater at Re ¼ 23,558 with 1.0% concentration and twist ratio of 5, compared to values with flow of water in a tube. An increase in the nanofluid concentration to 3.0% decreased heat transfer coefficients to values lower than water for flow in a tube and with tape inserts. A thermal system with tape insert of twist ratio 15 and 1.0% TiO_2 concentration gives maximum advantage ratio, if pressure drop is considered along with enhancement in heat transfer coefficient.

Zamzamian et al(2013) studied experimentally Factor Effect Estimation in the Convective Heat Transfer Coefficient Enhancement of Al_2O_3-EG Nanofluid in a Double-pipe Heat Exchanger The forced convective heat transfer (CHT) coefficient of a particular nanofluid, Al_2O_3 nanoparticles-ethylene glycol (EG) mixture, was investigated experimentally in a double-pipe heat exchanger. Nusselt number of the nanofluid for different nanoparticle concentrations as well as various operating temperatures was found to increase up to 23.7% using 1.0% wt of nanoparticles. The significance and novelty of this work is that 22-screening design was used to investigate the effect of factors and the results emphasized that increasing nanoparticle concentration had considerable effect on the enhancement of CHT coefficient of nanofluid. The effect of temperature and concentration of nanoparticles on nanofluid *Nu* number were inquired. They found convective heat transfer coefficient increases by increasing the temperature and nanoparticle concentration so the greatest *Nu* number was yielded at 75°C and 1.0 wt% of alumina nanoparticles. They tried to validate the correlation:

$$Nu=(h*d/k)=.4328(1.0+11.285\varphi^{0.754}Pe_p^{0.218})Re^{.0.333}Pr^{0.4} \quad (10)$$

In the deviations the found that the heat transfer coefficient of nanofluids was calculated from theoretical equations and compared with experimental results .The comparison of experimental results and semi empirical correlation results showed considerable deviations for high operating temperatures and nanoparticle concentrations.

Azmi et al (2014) did Experimental determination of heat transfer coefficients of SiO_2/water and TiO_2/water nanofluid up to 4% volume concentration flowing in a circular tube. The investigations were conducted in the Reynolds number range of 5000 to 25000 at a bulk temperature of 30^oC. The experiments are undertaken for flow in a circular tube with twisted

tapes of different twist ratios in the range of $5 < H/D < 93$. The heat transfer enhancement inversely increased with twist ratio. The heat transfer coefficient of SiO_2/water nanofluid at 3.0% volume concentration is 27.9% higher than water flow for the same twist ratio of five. However, the value of heat transfer coefficient of TiO_2/water nanofluid evaluated at the same concentration is 17.3% greater than water for twist ratio five. Regression equations for Nusselt number estimation are developed valid for water and nanofluid flow with twisted tape inserts under turbulent flow conditions. The equation developed is:

$$Nu=\frac{hD}{K}=.073Re^{0.702}Pr^{0.4}*(1+D/H)^{1.3} \quad (11)$$

The maximum heat transfer enhancement with twisted tape for TiO_2/water and SiO_2/water nanofluids was found at 1.0% and 3.0% volume concentration, respectively.

Luciu et al (2009) made a study into nusselt number and convection heat transfer coefficient for a coaxial heat exchanger using Al_2O_3–water, P_h=5 nanofluid. Performances of a particular nanofluid composed of aluminum oxide (Al_2O_3) particles dispersed in water for various concentrations ranging from 0 to 4% were investigated. The experimental set up is a coaxial exchanger, which is destined to solar application, in which the heating liquid used is the nanofluid studied. Experimental data have clearly shown a low Nusselt number due to the high conductivity number for this fluids, and high convection transfer coefficient. New measured data were also provided regarding the surface temperature. of the tube and not taking account only the bulk temperature to have a best representation of heat transfer in a laminar flow with this kind of fluid.

Balla et al (2013) studied enhancement of heat transfer coefficient multi-metallic nanofluid with ANFIS Modeling for Thermo physical Properties, Cu and Zn-water nanofluid is a suspension of

the Cu and Zn nanoparticles with the size 50 nm in the water base fluid for different volume fractions to enhance its Thermophysical properties. The determination and measuring the enhancement of Thermophysical properties depends on many limitations. Nanoparticles were suspended in a base fluid to prepare a nanofluid. A coated transient hot wire apparatus was calibrated after the building of the all systems. The vibro-viscometer was used to measure the dynamic viscosity. The measured dynamic viscosity and thermal conductivity with all parameters affected on the measurements such as base fluids thermal conductivity, volume factions, and the temperatures of the base fluid were used as input to the Artificial Neural Fuzzy inference system to modeling both dynamic viscosity and thermal conductivity of the nanofluids. Then, the ANFIS modeling equations were used to calculate the enhancement in heat transfer coefficient using CFD software. The heat transfer coefficient was determined for flowing flow in a circular pipe at constant heat flux. It was found that the thermal conductivity of the nanofluid was highly affected by the volume fraction of nanoparticles. A comparison of the thermal conductivity ratio for different volume fractions was undertaken. The heat transfer coefficient of nanofluid was found to be higher than its base fluid. Comparisons of convective heat transfer coefficients for Cu and Zn nanofluids with the other correlation for the nanofluids heat transfer enhancement are presented. Moreover, the flow demonstrates anomalous enhancement in heat transfer nanofluids Thermophysical properties predicted by the ANFIS model have a good agreement with the experimental measurements. The hybrid nanofluids present a good enhancement for the heat transfer coefficient with higher enhancement in the ratio for Cu is 40 % while for the Zn is 20% in comparison with water for volume fraction 1%.

Salehi et al(2013) did work on Nero-fuzzy modeling of the convection heat transfer coefficient for the nanofluid. In this study, experiments were performed by six different volume fractions of

Al2O3 nanoparticles in distilled water. Then, actual nanofluid Nusselt number compared by Adaptive Nero fuzzy inference system (ANFIS) predicted number in square cross-section duct in laminar flow under uniform heat flux condition. Statistical values, which quantify the degree of agreement between experimental observations and numerically calculated values, were found greater than 0.99 for all cases. The simulation results indicated that ANFIS model provided the reliable predictions for comparison with the experimental data. In almost all the train and test data studied with ANFIS models, %ARE, %AARE, MSE and RMSE calculated, these error values were achieved between 0.001 and 0.1 during training and testing process. Another salient aspect of the ANFIS modeling was that correct prediction to the tune of almost 100 % was achieved at the first training epoch. They deduced that fast convergence to optimality at the first epoch itself is due to the conjunction of the subtractive clustering with ANFIS. Finally they remarked that ANFIS is a promising predicting technique that would be effectively used for improved process to predict the Nusselt Number of the heat convection. Their study will be continued to increase the effectiveness of the proposed model by increasing and manipulating the content of the rules, data's and variables along with comparison with the other classical and intelligent techniques

Kulkarni et al., (2008) investigated heat transfer and fluid dynamic performance of nanofluids comprised of silicon dioxide (SiO2) nanoparticles suspended in a 60:40 (% by weight) ethylene glycol and water (EG/water) mixture. The heat transfer test section was a straight copper tube with outside diameter of 4.76 mm, inside diameter of 3.14 mm, and a length of 1 m. The wall temperature was measured by means of six thermocouples mounted on the tube surface along the length. The inlet and outlet temperatures of the nanofluid were measured using two thermowells

at the inlet and outlet of the test section. Two plastic fittings at inlet and outlet section of the copper tube provide a thermal barrier to axial heat conduction. The test section was heated electrically by four strip heaters to attain the Application of Nanofluids in Heat Transfer 421 constant heat flux boundary condition. The test section was insulated by 10 cm of fiber glass to minimize the heat loss from the heat transfer test system to ambient air. A four-pass shell and tube counter flow heat exchanger cools the nanofluids to keep the inlet fluid temperature constant using shop water. The effect of particle diameter (20 nm, 50 nm, 100 nm) on the viscosity of the fluid was investigated. They performed experiments to investigate the convective heat transfer enhancement of nanofluids in the turbulent regime by using the viscosity values measured. They observed increase in heat transfer coefficient due to nanofluids for various volume concentrations and loss in pressure was observed with increasing nanoparticle volume concentration.

Guzei et al (2014) studied experimentally measuring the Heat Transfer Coefficient of Nanofluid Based on Copper Oxide in a Cylindrical Channel. The studied nanofluid was prepared based on distilled water and CuO nanoparticles. Nanoparticle concentration varied in the range from 0.25 to 2% in the volume. The nanofluid was stabilized using a xan_ thane gum biopolymer the mass concentration of which did not exceed 0.03%. Considerable intensification of heat transfer was found. the heat transfer coefficient for a 1% nanofluid exceeds the corresponding value for water by more than 40% at almost any Re. The pump that was used in the experiments did not permit one to obtain consumptions exceeding 500 g/min. For this reason, for a 2% nanofluid, the obtained Reynolds numbers were only about 300. The dependence of the heat transfer coefficient for this nanofluid on the Reynolds number causes increase extremely steeply. Approximating the

dependence of the heat transfer coefficient on the Reynolds number for the 2% nanofluid, one can say with confidence that the excess of the heat transfer coefficient appears to be twofold or even larger. Certainly, this effect falls monotonically with a decrease in concentration of nanoparticles. When the value of the Reynolds number for water exceeds 2000, laminar–turbulent transition takes place, which intensifies its heat exchange. The nanofluid appeared to be Newtonian when particle concentrations exceeded 0.25%. Estimates for rheological parameters of the nanofluid and thermal conductivity coefficient have been obtained.

Ding et al., (2006) were first to study the laminar entry flow of water-based nanofluids containing multiwalled carbon nanotubes (CNT nanofluids). Significant enhancement in the convective heat transfer was observed in relation to pure water as the working fluid. The enhancement depends on the flow condition, CNT concentration and the pH level, and the effect of pH is observed to be small. They stated that the enhancement in convective heat transfer is a function of the axial distance from the inlet of the test section. This enhancement increases first, reaches a maximum, and then decreases with increasing axial distance. For nanofluids containing only 0.5 wt% CNTs, the maximum enhancement in the convection heat transfer coefficient reaches over 350% at Re = 800. Such a high level of enhancement could not be attributed purely to enhanced thermal conductivity. They proposed possible mechanisms such as particle rearrangement, reduction of thermal boundary layer thickness due to the presence of nanotubes, and the very high aspect ratio of CNTs. They also concluded that, the observed large enhancement of the convective heat transfer could not be attributed purely to the enhancement of thermal conduction under the static conditions. Particle re-arrangement, shear induced thermal conduction enhancement, reduction of thermal boundary layer thickness due to the presence of

nanoparticles, as well as the very high aspect ratio of CNTs are proposed to be possible mechanisms.

Rea et al. (2009) investigated laminar convective heat transfer and viscous pressure loss for alumina–water and zirconia–water nanofluids in a flow loop. The vertical heated test section was a stainless steel tube with an inner diameter (ID) of 4.5 mm, outer diameter (OD) of 6.4 mm, and length of 1.01 m. The test section had eight sheathed and electrically insulated Ttype thermocouples soldered onto the outer wall of the tubing along axial locations of 5, 16, 30, 44, 58, 89, 100 cm from inlet of the heated section. Two similar T-type thermocouples were inserted into the flow channel before and after the test section to measure the bulk fluid temperatures. The heat transfer coefficients in the entrance region and in the fully developed region were found to increase by 17% and 27%, respectively, for alumina–water nanofluid at 6 vol % with respect to pure water. The zirconia–water nanofluid heat transfer coefficient increases by approximately 2% in the entrance region and 3% in the fully developed region at 1.32 vol %. The measured pressure loss for the nanofluids was in general much higher than for pure water and in good agreement with the traditional model predictions for laminar flow

Heriz et al. (2006) investigated laminar flow convective heat transfer through circular tube with constant wall temperature boundary condition for nanofluids containing CuO and Al_2O_3 oxide nanoparticles in water as base fluid. The experimental apparatus consisting of a test chamber constructed of 1 m annular tube with 6 mm diameter inner copper tube and with 0.5 mm thickness and 32 mm diameter outer stainless steel tube. Nanofluid flows inside the inner tube while saturated steam enters annular section, which creates constant wall temperature boundary

condition. The fluid after passing through the test section enters heat exchanger in which water was used as cooling fluid. The experimental results emphasized that the single phase correlation with nanofluids properties (Homogeneous Model) was not able to predict heat transfer coefficient enhancement of nanofluids. The comparison between experimental results obtained for CuO/ water and Al2O3 / water nanofluids indicated that heat transfer coefficient ratios for nanofluid to homogeneous model in low concentration were close to each other but by increasing the volume fraction, higher heat transfer enhancement for Al2O3/water was observed. They concluded that heat transfer enhancement by nanofluid depends on several factors including increment of thermal conductivity, nanoparticles chaotic movements, fluctuations and interactions

Hojjat et al. (2011) experimentally investigated the forced convection heat transfer of non-Newtonian nanofluids in a circular tube with constant wall temperature under turbulent flow conditions. Three types of nanofluids were prepared by dispersing homogeneously-Al_2O_3, TiO_2 and CuO nanoparticles into the base fluid. An aqueous solution of carboxymethylcellulose (CMC) was used as the base fluid. Nanofluids as well as the base fluid show shear thinning (pseudo plastic) rheological behavior. The test section consists of two 2-m long concentric tubes. The internal diameter of inner tube was 10 mm and a thickness 2 mm. The internal diameter of outer tube was 48 mm. Both tubes were made of stainless steel (type 316). The nanofluid flows through the inner tube whereas hot water was circulated through the annular section at high flow rates in order to create constant wall temperature boundary condition. Results indicated that the convective heat transfer coefficient of nanofluids is higher than that of the base fluid. The enhancement of the convective heat transfer coefficient increases with an increase in the Peclet

number and the nanoparticle concentration. The increase in the convective heat transfer coefficient of nanofluids was greater than the increase that would be observed considering strictly the increase in the effective thermal conductivity of nanofluids. Experimental data were compared to heat transfer coefficients predicted using available correlations for purely viscous non-Newtonian fluids. Results showed poor agreement between experimental and predicted values. Hence they proposed a new correlation (Eq.26) to successfully predict Nusselt numbers of non-Newtonian nanofluids as a function of Reynolds and Prandtl numbers.

Pathipakka and Sivashanmugam (2010) numerically estimated the heat transfer behavior of nanofluids in a uniformly heated circular tube fitted with helical inserts in laminar flow. They used Al2O3 nanoparticles in water of 0.5%, 1.0% and 1.5% concentrations and helical twist inserts of twist ratios (ratio of length of one twist to diameter of the twist) 2.93, 3.91 and 4.89 for the simulation. Assuming the nanofluid behave as a single phase fluid, they investigated three dimensional steady state heat transfer behavior using fluent 6.3.26. They concluded that the heat transfer increases with Reynolds number and decrease in twist ratio with maximum for the twist ratio 2.93. The increase in Nusselt number was 5%_31% for\ helical inserts of different twist ratio and nanofluids of different volume concentrations. The heat transfer enhancement was 31% for helical tape insert of twist ratio 2.93 and Al2O3volume concentration of 1.5% corresponding to the Reynolds number of 2039.

$$Nu = 0.279 (\mathrm{ReP r})_{nf}^{0.558} \left(\frac{p}{d}\right)^{-0.447} (1+\varphi)^{134.65}$$

$$\mathbf{Nu=.279(Re*Pr)_{nf}^{0.558}*(p/d)^{-0.447}*(1+\varphi)^{134.65}}$$

Xuan and Li (2003) built an experimental rig to study the flow and convective heat transfer feature of the nanofluid flowing in a tube. Their test section was a straight brass tube of the inner diameter of 10 mm and the length of 800 mm. Eight thermocouples were mounted at different places of the heat transfer test section to measure the wall temperatures and other two thermocouples were respectively located at the entrance and exit of the test section to read the bulk temperatures of the nanofluid. They investigated convective heat transfer feature and flow performance of Cu-water nanofluids for the turbulent flow. The suspended nanoparticles remarkably enhance heat transfer process and the nanofluid has larger heat transfer coefficient than that of the original base liquid under the same Reynolds number. They found that at fixed velocities, the heat transfer coefficient of nanofluids containing 2.0 vol% Cu nanoparticles was improved by as much as 40% compared to that of water. The Dittus–Boelter correlation failed to predict the improved experimental heat transfer behavior of nanofluids. The heat transfer feature of a nanofluid increases with the volume fraction of nanoparticles. They have proposed the following correlation:

$$Nu=0.0059(1+7.6286\varphi^{0.6886}Pe^{0.001})Re^{0.9238}Pr^{0.4} \quad (12)$$

Maiga et al., (2005) presented the numerical study of fully developed turbulent flow of Al_2O_3 - water nanofluid in circular tube at uniform heat flux of 50 W/cm^2. The following correlations have been proposed for computing the averaged Nusselt number for the nanofluids considered for both the thermal boundary conditions, valid for Re <1000, 3<Pr < 7.53 and φ< 10%

$$Nu=0.086Re^{0.55}Pr^{0.5} \quad (13)$$

The classical k-φ model was used for turbulence modeling and their study clearly showed that the inclusion of nanoparticles into the base fluids has produced a considerable augmentation of the heat transfer coefficient that clearly increases with an increase of the particle concentration. However, the presence of such particles has also induced drastic effects on the wall shear stress that increases appreciably with the particle loading. Among the mixtures studied, the ethylene glycol γ- Al_2O_3nanofluid appears to offer a better heat transfer enhancement than water– γ- Al_2O_3.

Chapter 3

Experimental setup, procedure and results

:

3.1.1 Experimental setup

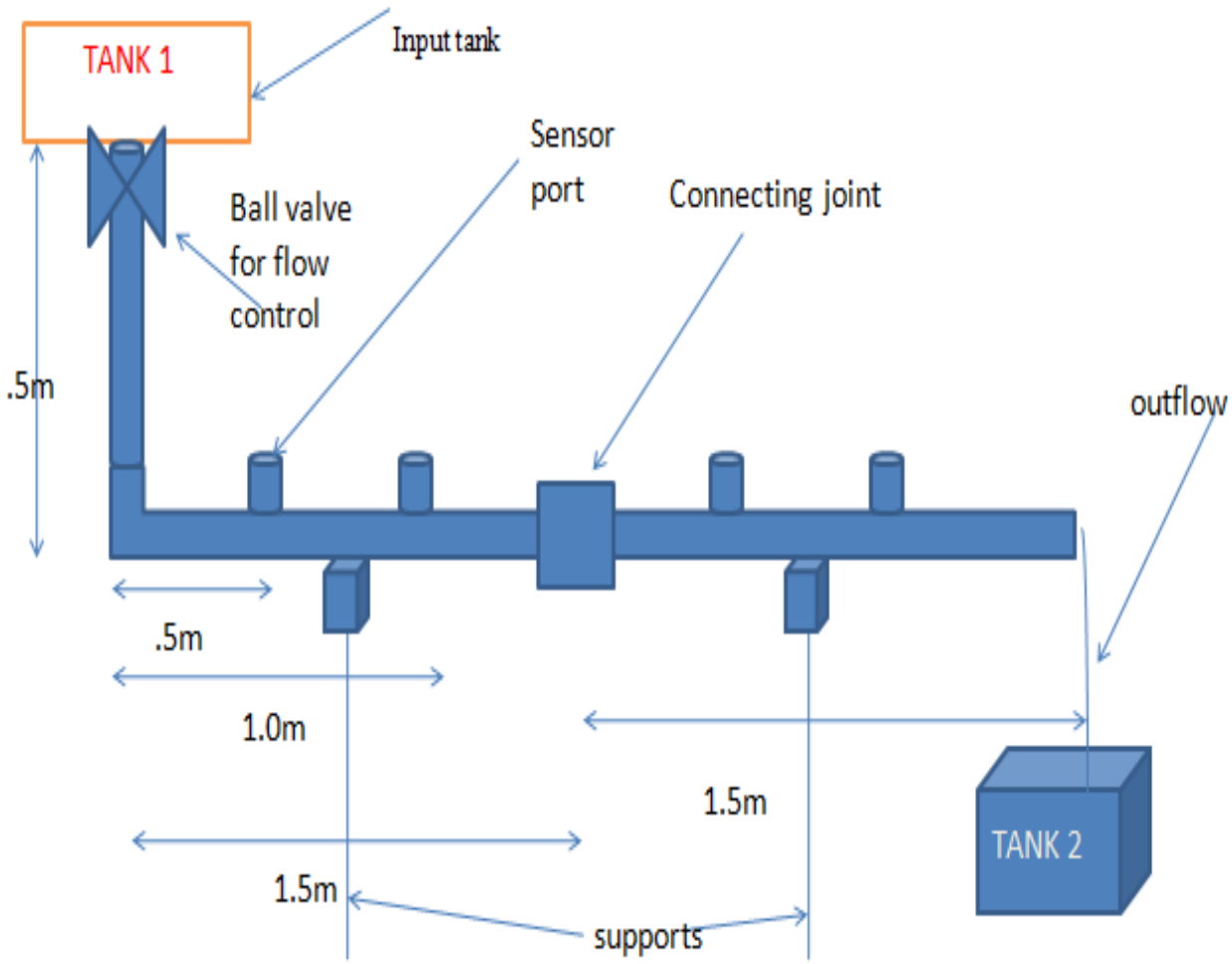

Figure 3.1.1 Experimental setup for flow under gravity and measurement of temperature

3.1.1 Calibration of setup with results of experiments on water:

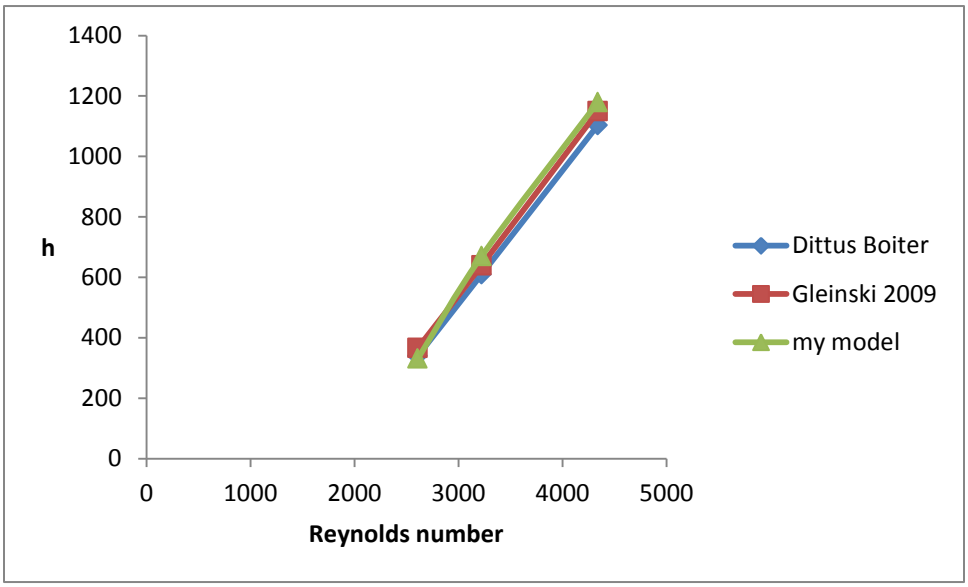

Figure 3.1.2: comparison of models for water at 3 different diameters and mass flow rates

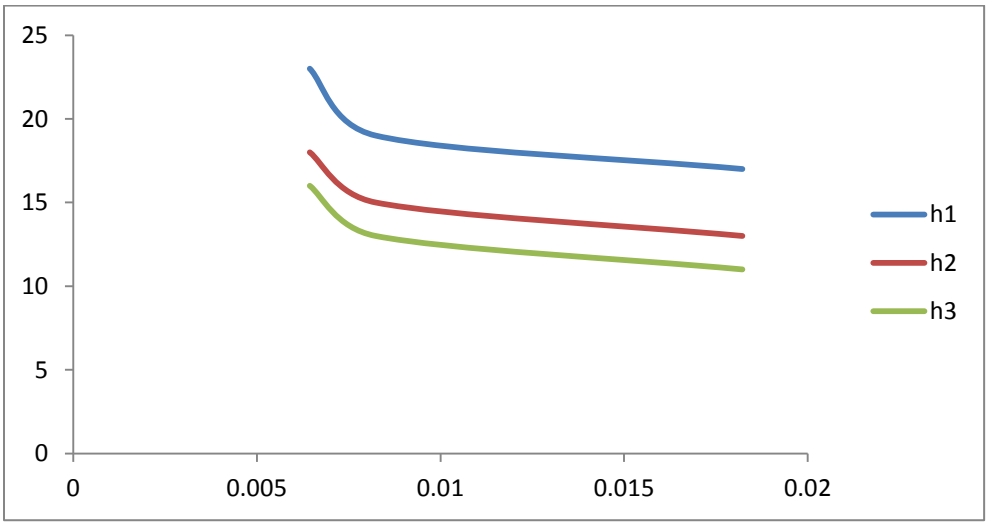

Figure 3.1.3:Mass flow vs h for water at 15.875mm diameter

.

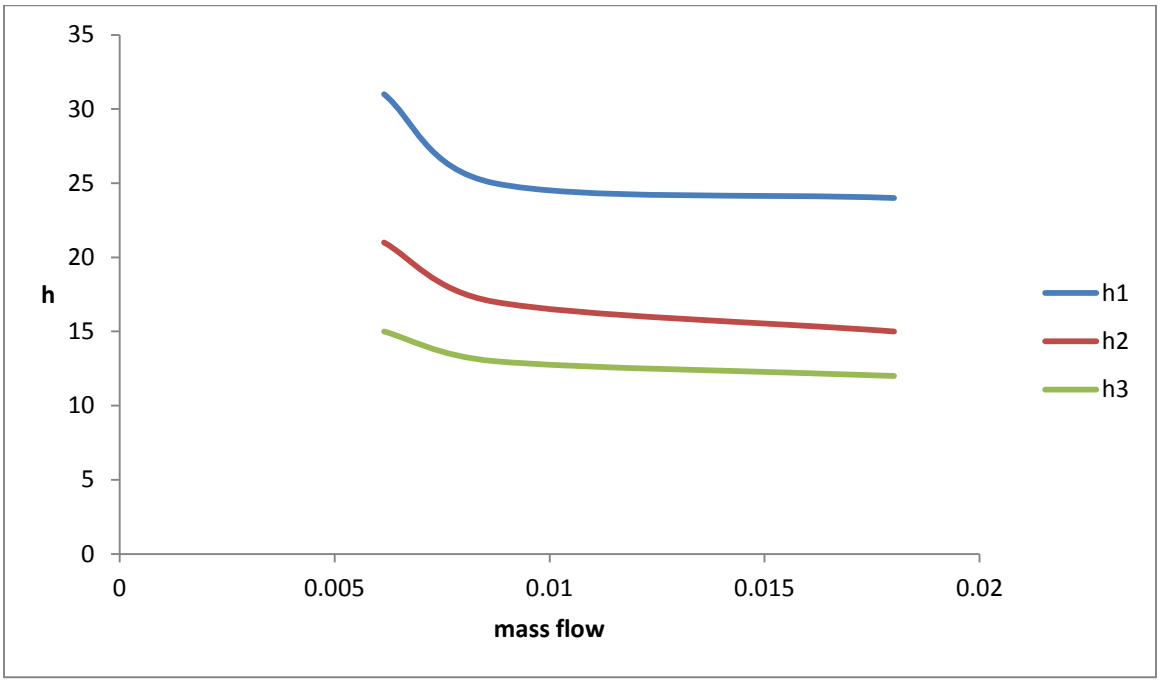

Figure 3.1.4: mass flow vs h of water at 12.7 mm

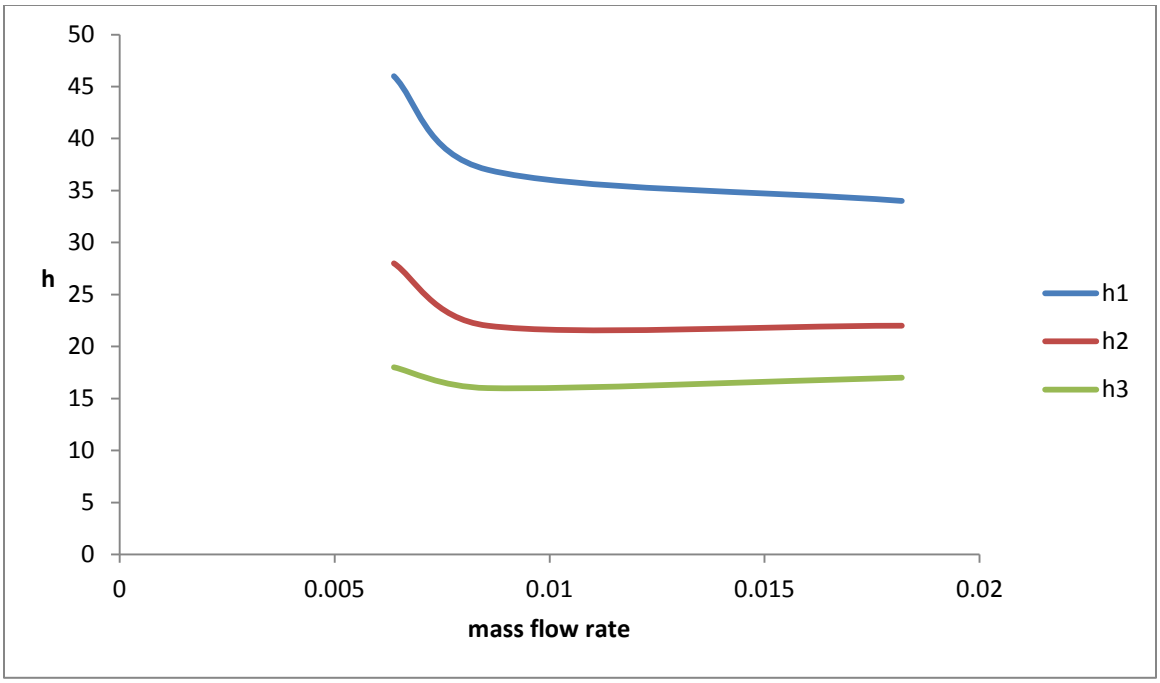

Figure 3.1.5: Mass flow vs h for water at 9.52 mm dia

3.1.2 Components of experimental setup:

Storage tanks: two tanks, one for input and other for output were used. the input tank was insulated with foam and reflective metal foil wrap to maintain constant temperature. the capacity of input tank is 8 liters and output tank is 10 liters.

Temperature sensors: 4 pt 100 platinum resistance type sensors with rage from -50 to 200°C.these sensors were attached to a display panel of indicator box. The box had a switch to change the sensor.

Copper pipes: Three copper pipes of diameters 9.525 mm, 12.7mm, 15.875 mm were used. The thickness 1mm.each diameter pipe had been used in two parts of 1.5m each. These parts are joined by flare nut joint. These pipes have 6mm dia ports that are 5 in number and at equal distances. These ports are opened to insert temperature measuring end of the temperature sensor.

Ball valve: a ball valve used to vary the mass flow rate by changing the area of constriction. a measuring flask and a stopwatch were used to measure the volume flow rate that was later converted to mass flow rate by multiplying with density.

Nanofluids: three different nanofluids of volume fraction of .01% were used. Three nanofluids used were Al_2O_3, CuO, and TiO_2. All of them were of size around 30nm. They were prepared by chemical precipitation. They were dispersed using bath type ultrasonicator. The sonication time was around 6 hrs. They were heated using oil bath to get desired initial state for heat loss experiments.

(i)Preparation of nanoparticles: Nanoparticles were prepared using Forced Hydrolysis for Oxides

Oxides are more stable thermally and chemically

Hydrolysis and condensation of metal salts with addition of catalysts (acids, bases)

$Si(OR)_4$ + (alcohol + NH_3 + H_2O) → 50nm-2μm SiO_2

$FeCl_3$ + HCl +H_2O at 95-99oC → 24h aging → quenching

Dilution required high supersaturation Ostwald ripening

Diffusional growth

$FeCl_2/FeCl_3$ + NH_4OH with dextran→ Fe_3O_4

Y_2NO_3 + Eu_2O_3 + H_2O + $(NH_2)_2CO$ → Y_2O_3

(ii)preparation of nanofluid: Ultrasonic bath was used to sonicate nanofluids due to large volume of nanofluid required. The bath had following features:

Capacity = 9.5 liters

Size = 15.6*15.8*14.9 (inches)

Frequency= 40 Hz

Sonication time= 5 hrs

3.1.3 Experimental procedure:

1) First the water or nanofluids were heated to desired temperature in ultrasonic bath and then put into input tank and then ball valve was opened to allow flow at desired mass flow rate.
2) The three different temperatures of around 55, 50 and 45 °C were used for each mass flow rate and three different mass flow rates were used for each pipe diameter.
3) The pipes were flushed thoroughly with water after each nanofluid so that they stayed clean for accurate results.
4) joints were checked for leakages
5) ambient conditions kept similar due with no change in atmospheric temperature in month of late may and no wind fluctuations

6) mass flow rate was measured indirectly by measuring volume flow rate(VFR) in ml/sec. the VFR was measured using a borosil flask and a stop watch. To get a better average 7 readings were taken, and then their average was taken as final VFR

7) the VFR was changed to mass flow rate by multiplying with density of nanofluid.

.

3.2Results:

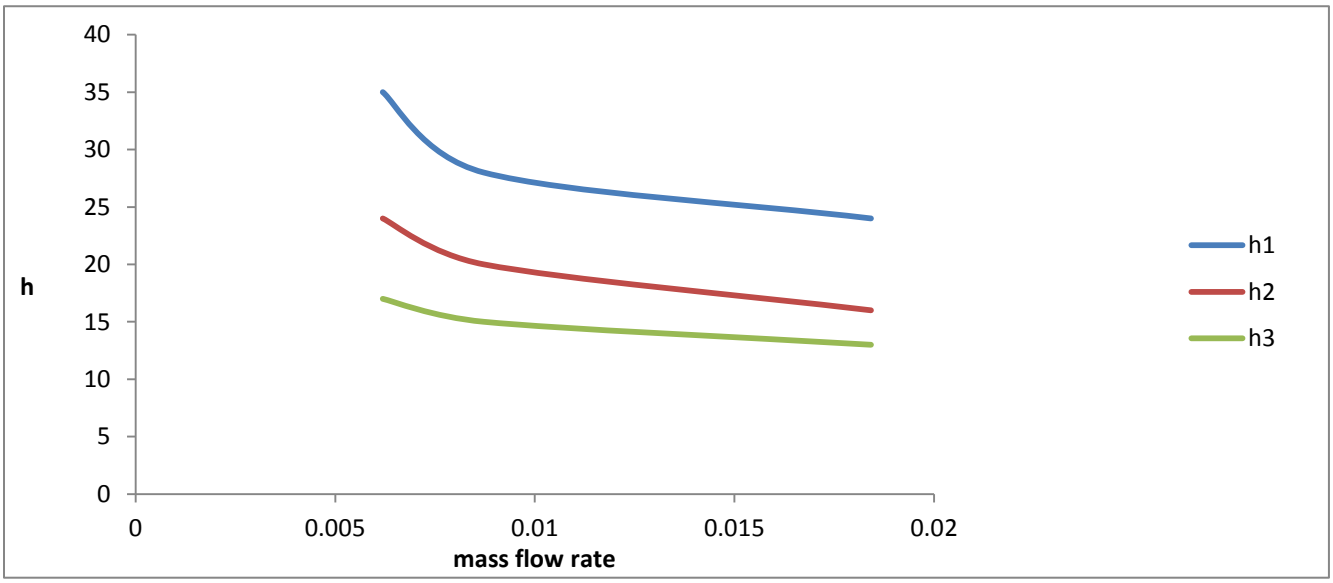

Figure 3.2.1:General Trend line for variation of mass flow rate vs. heat transfer coefficient in observed readings for different nanofluids

Above and everywhere in this work:

h_1 represents variation when initial temperature is around 55°C.

h_2 represents conditions with 50°C as initial temperature.

h_3 represents conditions with 45°C as initial temperature.

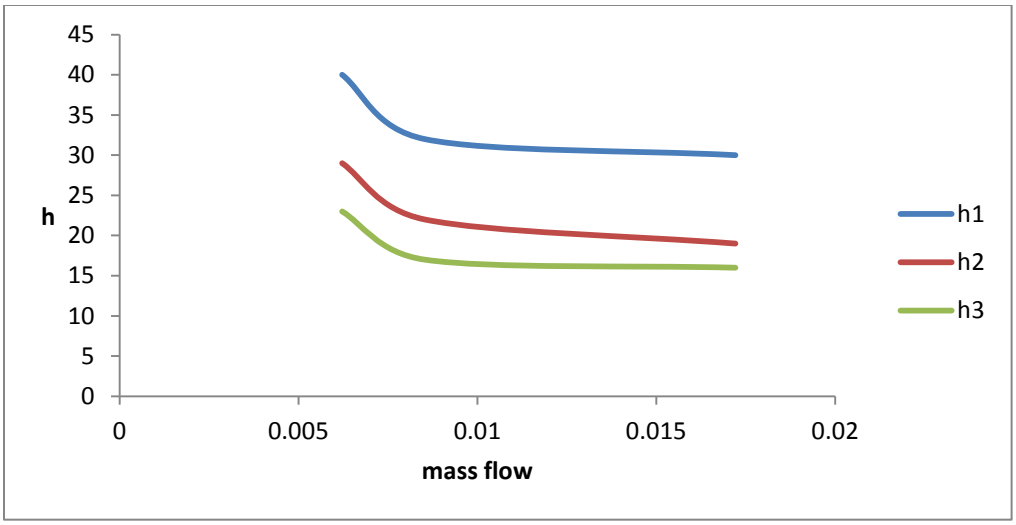

Figure 3.2.2: mass flow vs h at 12.7 mm diameter for CuO

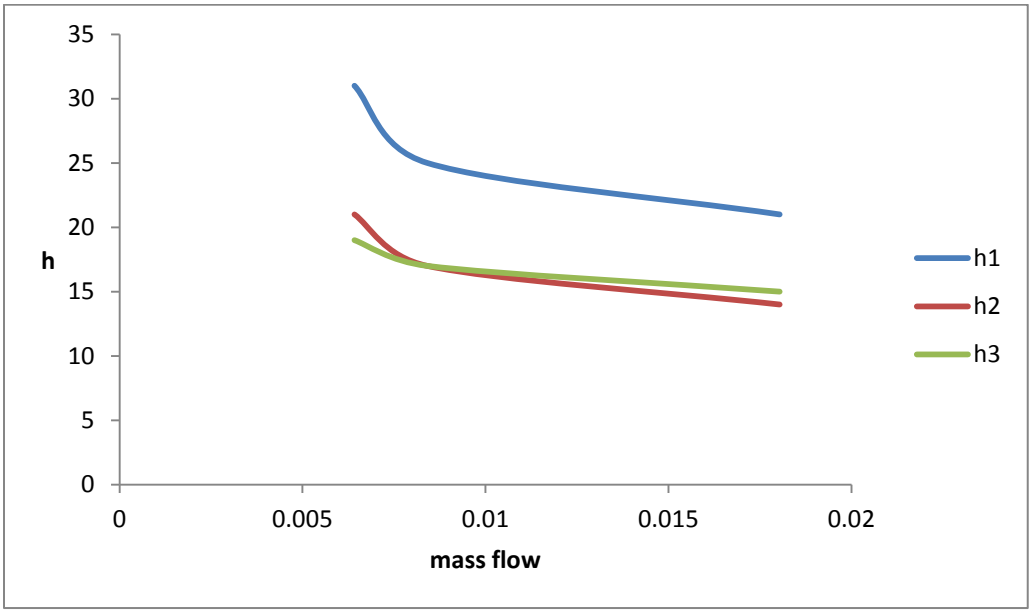

Figure 3.2.3: mass flow vs. h at 15.875 mm diameter for alumina

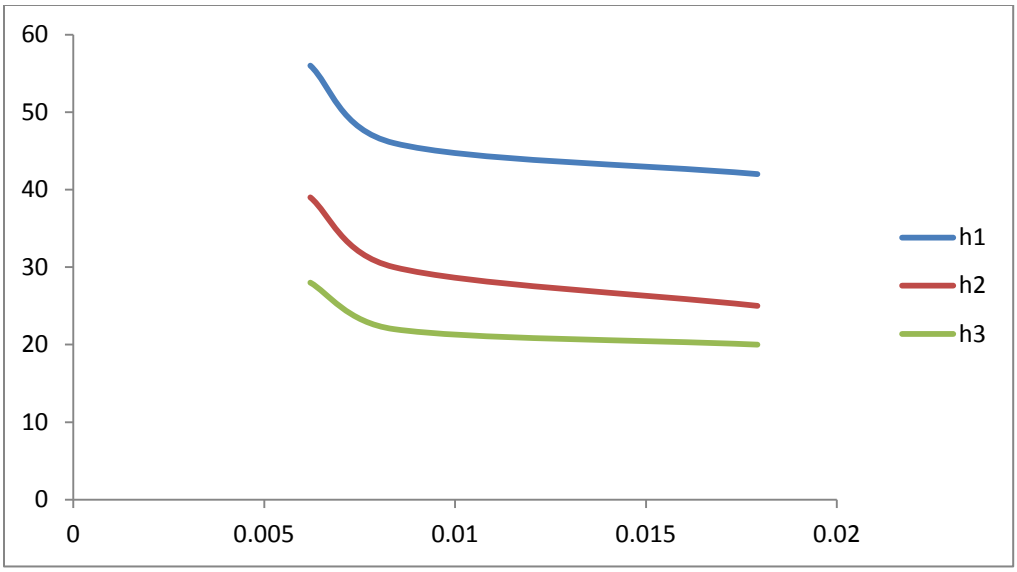

Figure 3.2.4: mass flow vs. h at 9.52mm diameter for alumina

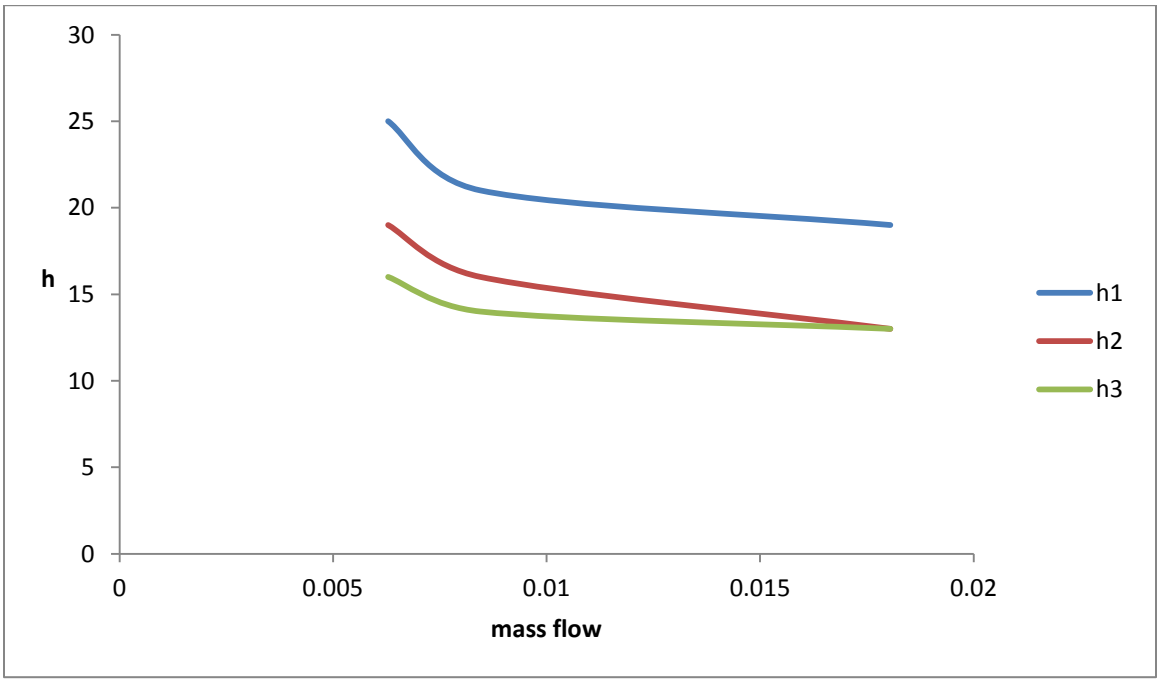

Figure 3.2.5 :mass flow vs. h at 15.875 mm for titanium dioxide.

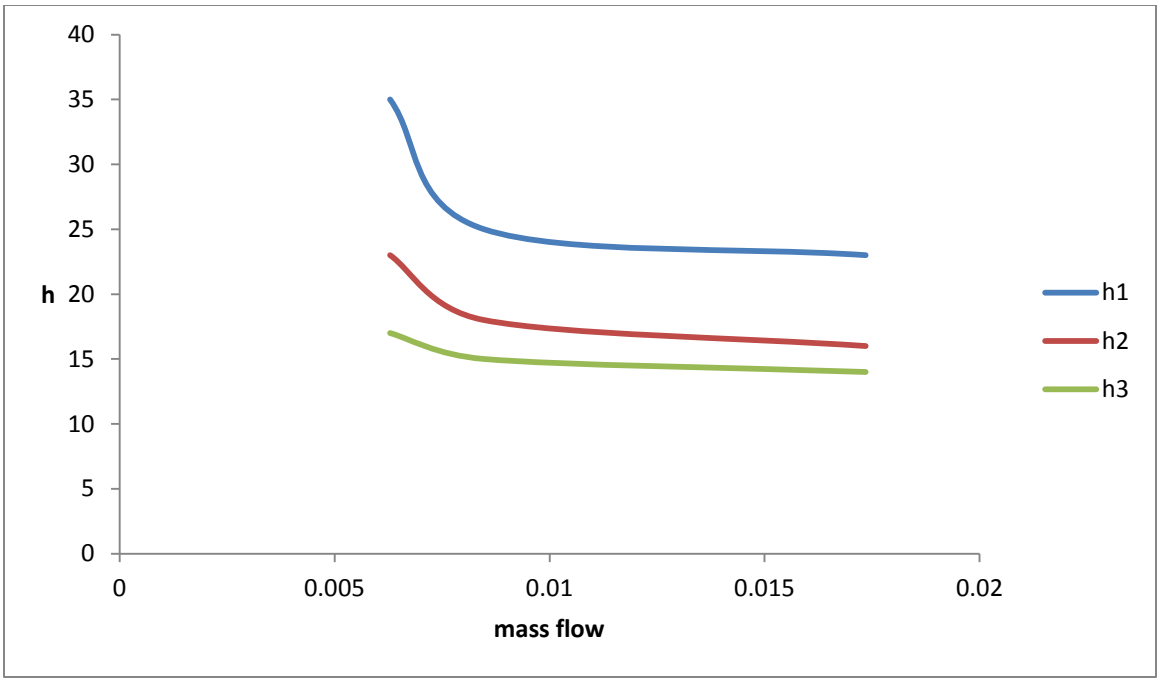

Figure 3.2.6: mass flow vs h at 12.7 mm diameter for titanium oxide.

For graphs 1-6: These graphs show a variation of heat transfer coefficient with change in mass flow rate at a constant diameter for a given nanofluid. we can observe that at high initial temperature the h.t coefficient is high with increased mass flow rate it reduces more than the case in which initial temperature is low. All the graphs follow similar trend to some error of 5%-10%.

3.3 Variation of nusselt no with Reynolds number

For graphs (3.3.1 - 3.3.3) the term

Nu1 means Nusselt number at 15.875 mm dia of pipe

Nu2 means Nusselt number at 12.7 mm dia of pipe

Nu3 means Nusselt number at 9.525 mm dia of pipe

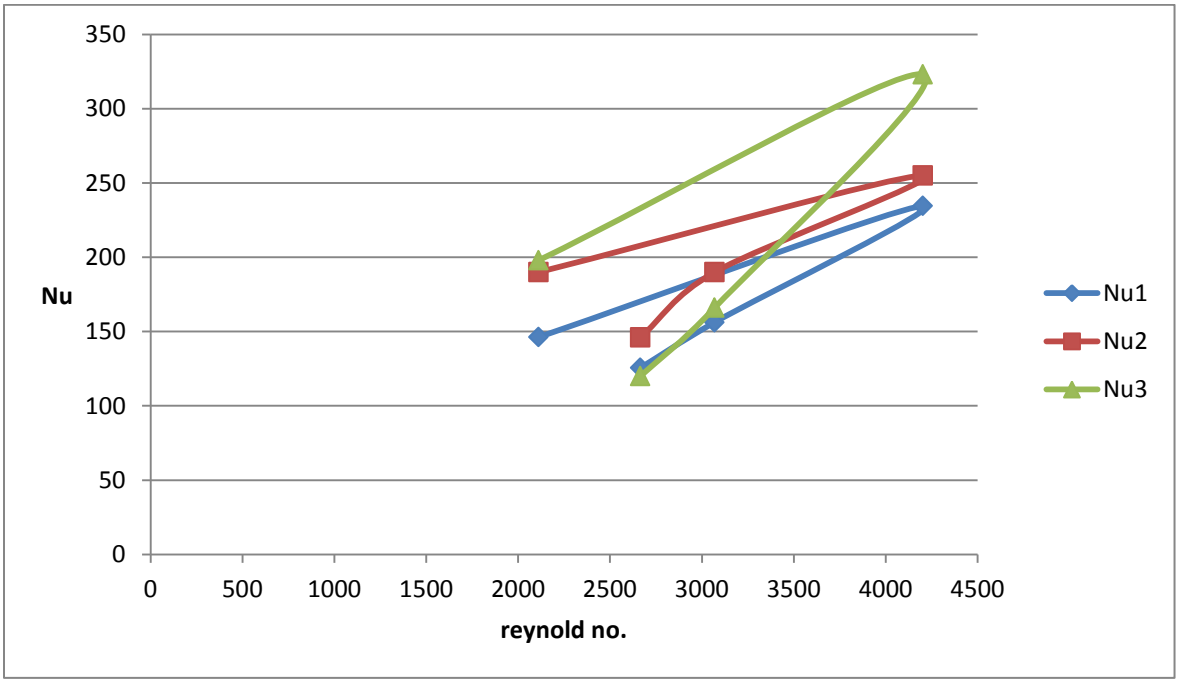

Figure 3.3.1:Nusselt number vs Reynolds no for copper oxide at diffent diameters.

Figure 3.3.2:Nusselt number vs Reynolds no for aluminum oxide at different diameters

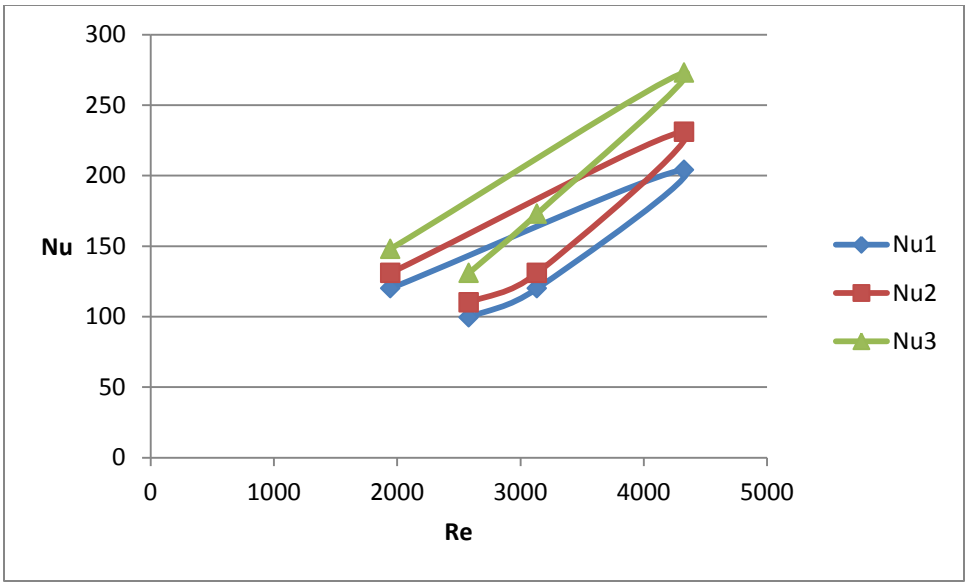

Figure 3.3.3:Nusselt number vs Reynolds no for Titanium oxide at different diameters

The above figures() show variation of nusselt number with Reynolds at different diameters of pipe and at different flow rates for same nanofluid of same concentration. The downtrend in curve can be attributed to decrease in diameter of pipe which leads to more filling of small diameter pipe for same mass flow rate as large diameter pipe which leads to more laminar flow. The variation or deviation from each other is maximum in case of copper oxide, followed by titanium oxide and least in case of aluminum oxide.

3.4 Varitation of nusselts number with change in Prandtl number

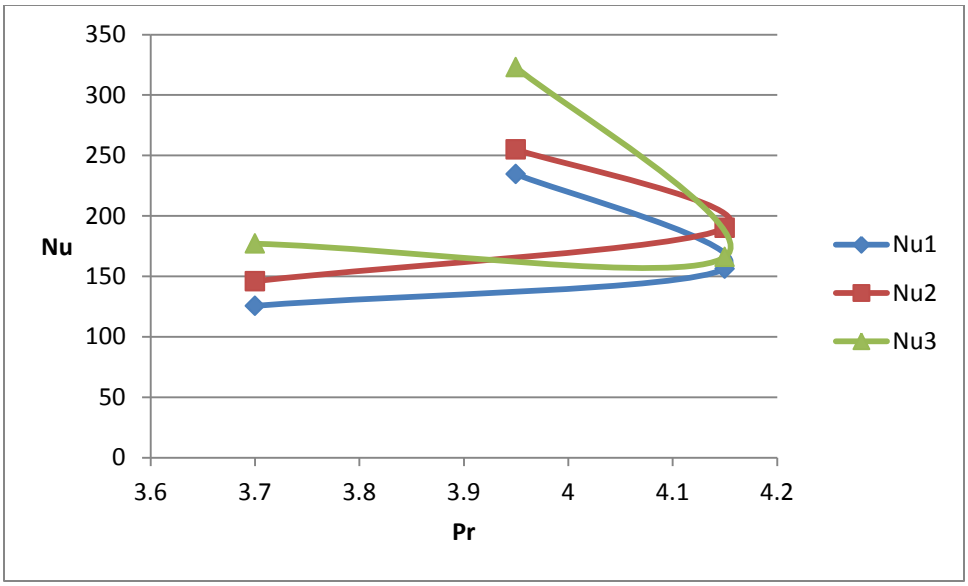

Figure 3.4.1 Nusselt number vs Prandtl number for copper oxide at different diameters

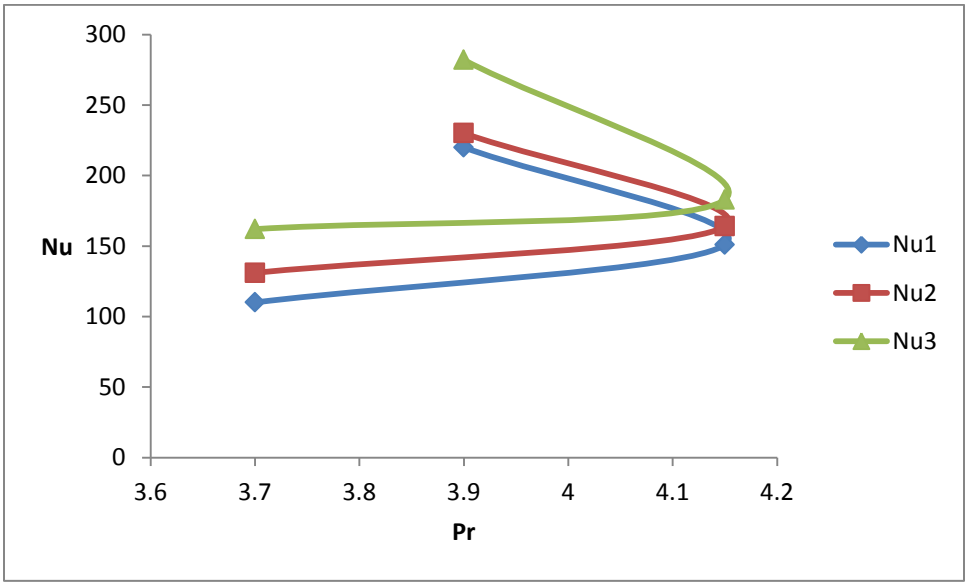

Figure 3.4.2: variation for aluminum oxide at different diameters

The figures () depict variation of nusselt number with Prandtl number for different diameters of same nanofluid of same concentration. The trend show continuous increase in nusselt number with increase in Prandtl number. This is consistent with most of non-Newtonian fluids.

3.5 Variation of temperature drop with change in nanofluids over same diameter

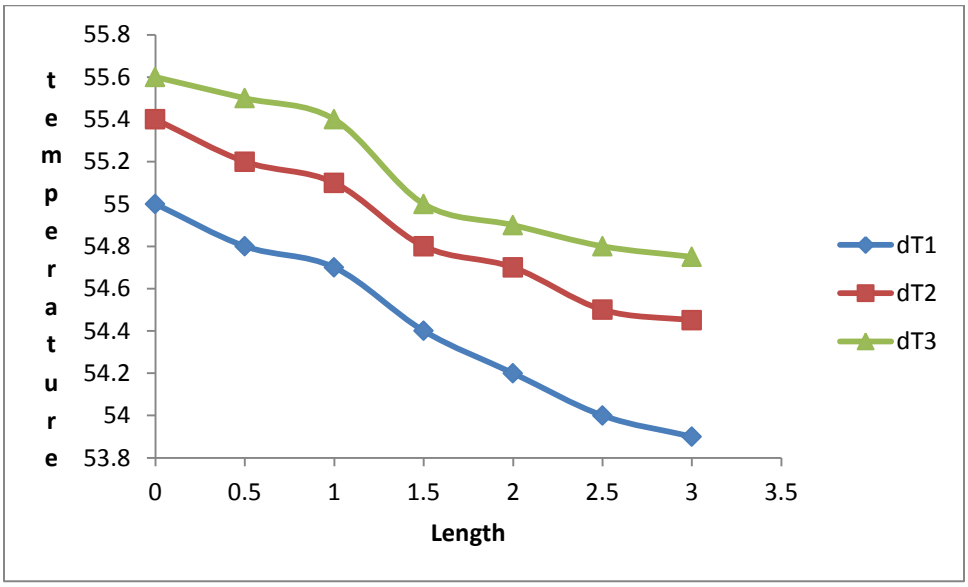

Figure 3.5.1 Variation graph atr 15.875mm diameter for all nanofluids

For figure(3.5.1-3.5.3) the legend is:

dT1= temperature drop for copper oxide at same diameter

dT2= temperature drop for aluminum oxide at same diameter

dT3= temperature drop for copper oxide at same diameter.

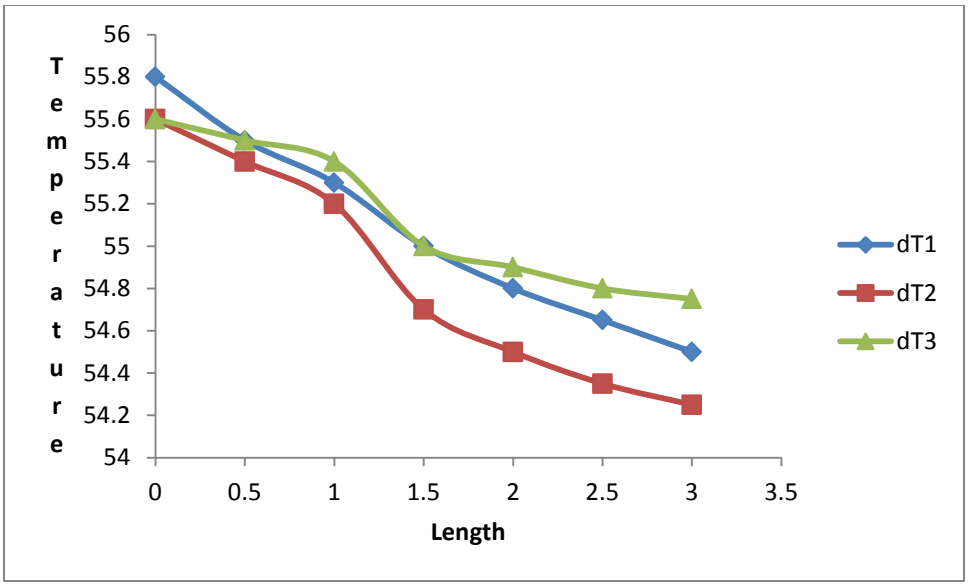

Figure 3.5.2 Variation graph at 12.7 mm diameter of pipe for all nanofluid

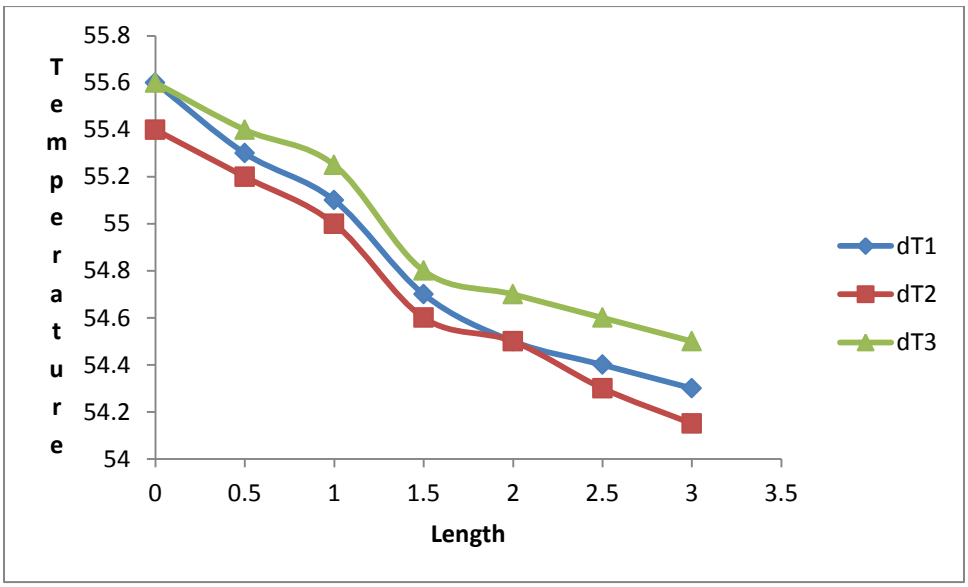

Figure 3.5.3 Variation graph for 9.525mm diameter of pipe for all nanofluids.

The above figures show variation of temperature drop with change of nanofluid for same diameter of pipe and same mass flow rate. The temperature drop is maximum at 9.525mm diameter, decreases in 12.7mm diameter pipe and is minimum in 15.875mm diameter pipe. It is due to more surface of contact of fluid in smaller pipe as the mass flow rate is constant.

3.6 Validation of model by comparing it with other authors models:

In this work the data in range of Reynolds number above 1900 was tested for this model. They varied by max 10%+_ from the theoretical models. The variation can be due to turbulence in cases with Reynolds number above 4000 and also due to different levels of fluid across the pipe

the density and viscosity of nanofluids were found using following correlations:

$$\rho_{nf}=\varphi\rho_p+(1-\varphi)\,\rho_f \quad (14)$$

$$\mu_{nf}=\mu_f(1+2.5\,\varphi) \quad (15)$$

and conductivity was calculated by correlation given by koo and Kleinstreuer(2004) :

$$K_{nf}\left(\frac{Kp+2Kf+2(Kp-Kf)\varphi}{Kp+2Kf-2(Kp-Kf)\varphi}\right)K_f \quad (16)$$

mallick proposed that a more accurate model using more variables like Gleninski model(2009) should be used for prediction of nusselt number. It is given by

$$\text{Nu}=\frac{hD}{K}=\left(\frac{f/2(\text{Re}-10^3)\text{Pr}}{1+12.7(f/2)^{0.5}(Pr^{.66}-1)}\right)(1+\frac{D^{.66}}{L^{.66}}) \quad (16)$$

Pak and cho (1998) model is given by:

$$\text{Nu}=0.021\text{Re}^{0.8}\ \text{Pr}^{0.5} \quad (17)$$

Zamzamian et al (2013) gave folowing model:

$$\text{Nu}=(h*d/k)=.4328(1.0+11.285\varphi^{0.754}\text{Pe}_p^{0.218})\text{Re}^{.0.333}\text{Pr}^{0.4} \quad (18)$$

The graph to compare Reynolds number vs. value of predicted heat transfer coefficient from these model for a 3m long pipe is given below

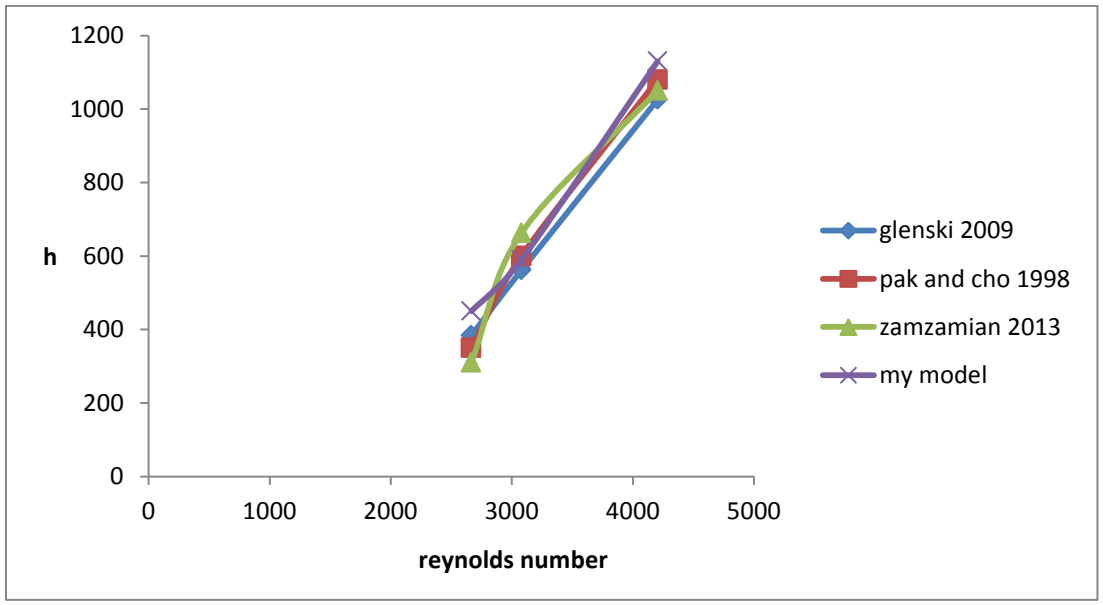

Figure 3.6.1 : Comparison of models for copper oxide at 3 different diameters and mass flow rates

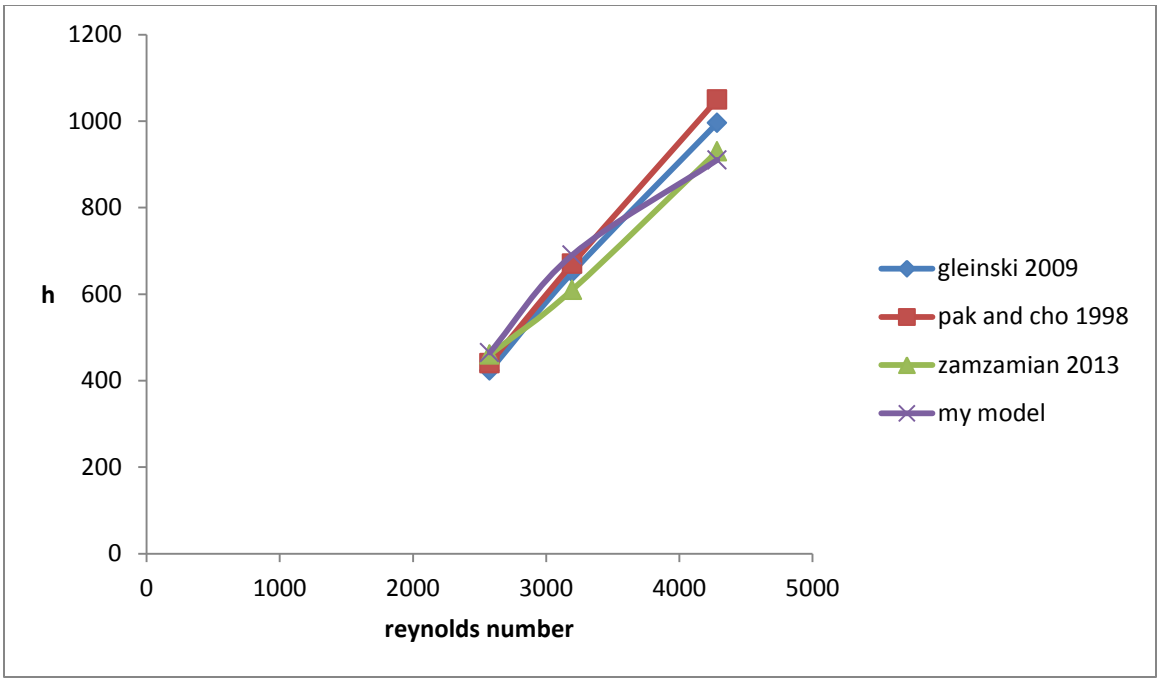

Figure 3.6.2 : comparison of models for aluminiumr oxide at 3 different diameters and mass flow rates

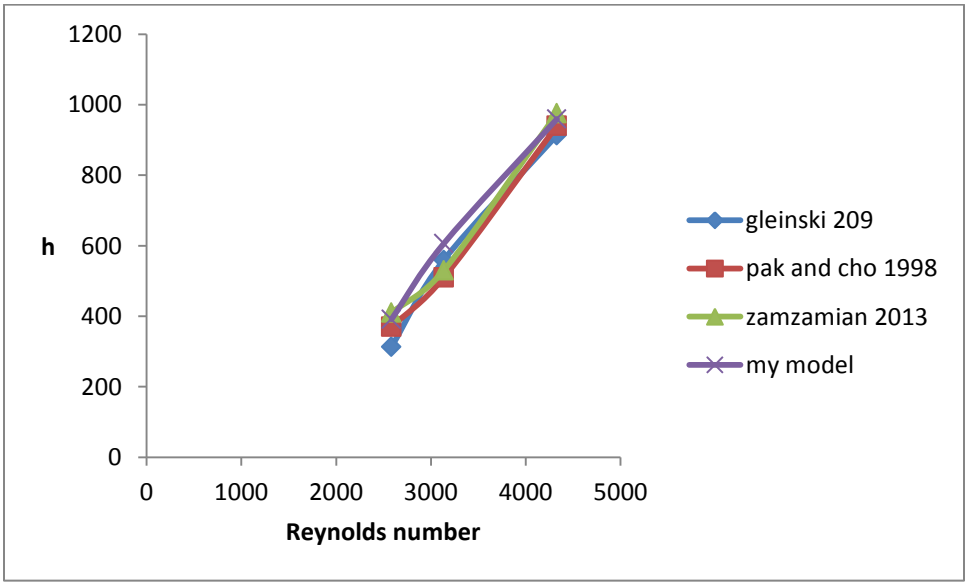

Figure 3.6.3: comparison of models for titanium oxide at 3 different diameters and mass flow rates

From above figures (3.6.1-3.6.3) we can see the comparison for Reynolds number vs heat transfer coefficient h for same nanofluid at different diameters and mass flow rates. These models differ from each other by error of 5-15%. The reason for this can be the parameters selected for model. E.g. Pak and Cho(1998) selected Re and Pr only as parameters. Gleninski et al(2009) used friction factor, and ratio diameter to tube length in additions to these parameters. My model used ratio of diameter of particle to pipe diameter and ratio of particle density to nanofluid density as parameters in addition to Re and Pr.

Chapter 4

Conclusion and future scope of work

4.1 Conclusion

This work done to evaluate the variation of heat transfer coefficient with mass flow, temperature of fluid and diameter shows that the velocity plays significant role in heat transfer enhancement and so does the diameter of pipe. The pipes with lesser diameters got more temperature drop due to reason that under the same mass flow rate they were running full with fluid and were exposing more surface area than larger pipes directly to fluid. an improvement of 5-10 % over water in heat transfer is observed.. The model developed from use of 3 different nanofluids at 0.01%volume fraction is dependent on ratio of particle diameter to pipe diameter and on the ratio of particle density to fluid density. So the derived model is dependent on different parameters than found in most of literature. It gives error of 5-15% when compared with other models dependent on different parameters. To eradicate this error further research can be done on to find other parameters that influence the convection heat transfer coefficient

4.2 Future Scope of work:

1) Heat transfer coefficient (HTC) is a better indicator in evaluate of thermal performance of the fluid. Thus, it is really important to know how to get the value of HTC since it is not a property of the fluid and it is experimentally determine parameter whose value depends on all variables influencing convection such as the surface geometry, the nature of fluids motion, and the properties of the fluid and bulk fluid velocity.
2) Design of nanofluid based heat exchangers
3) Improvement of model derived from the experimental data similar to this work.

Appendix

Appendix A

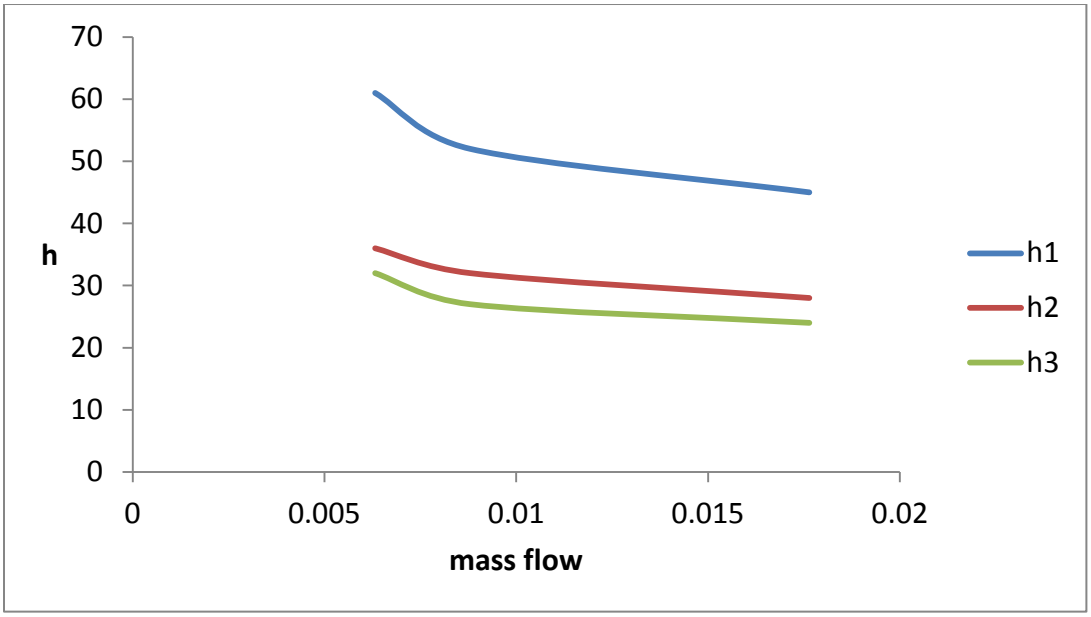

Figure A1: mass flow vs. h for 9.52mm pipe for CuO

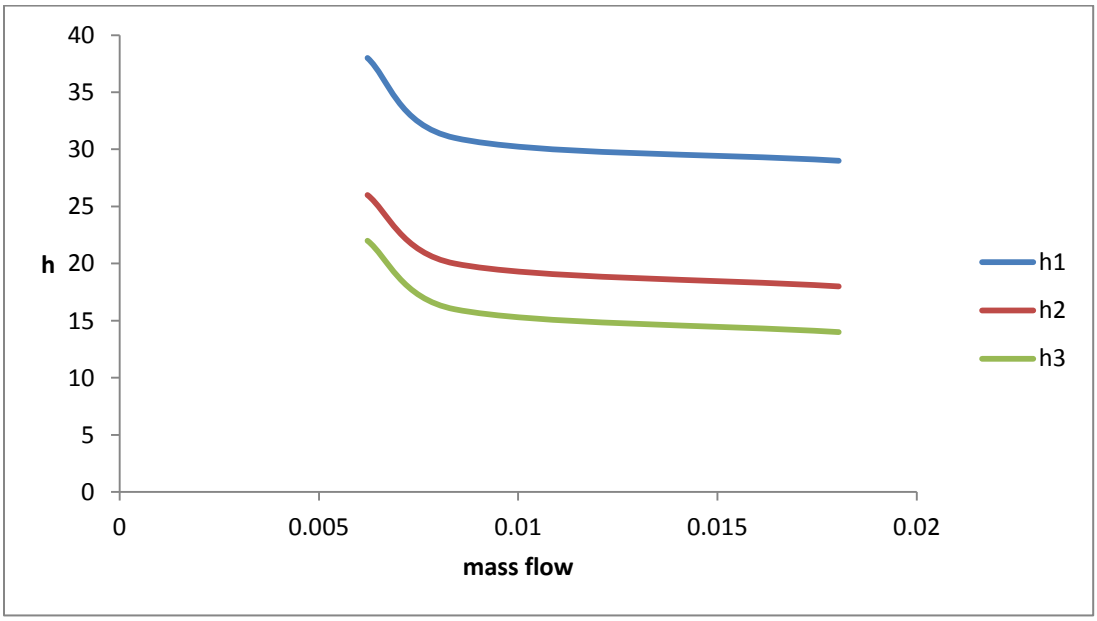

FigureA2: mass flow vs h at 12.7 mm dia for alumina

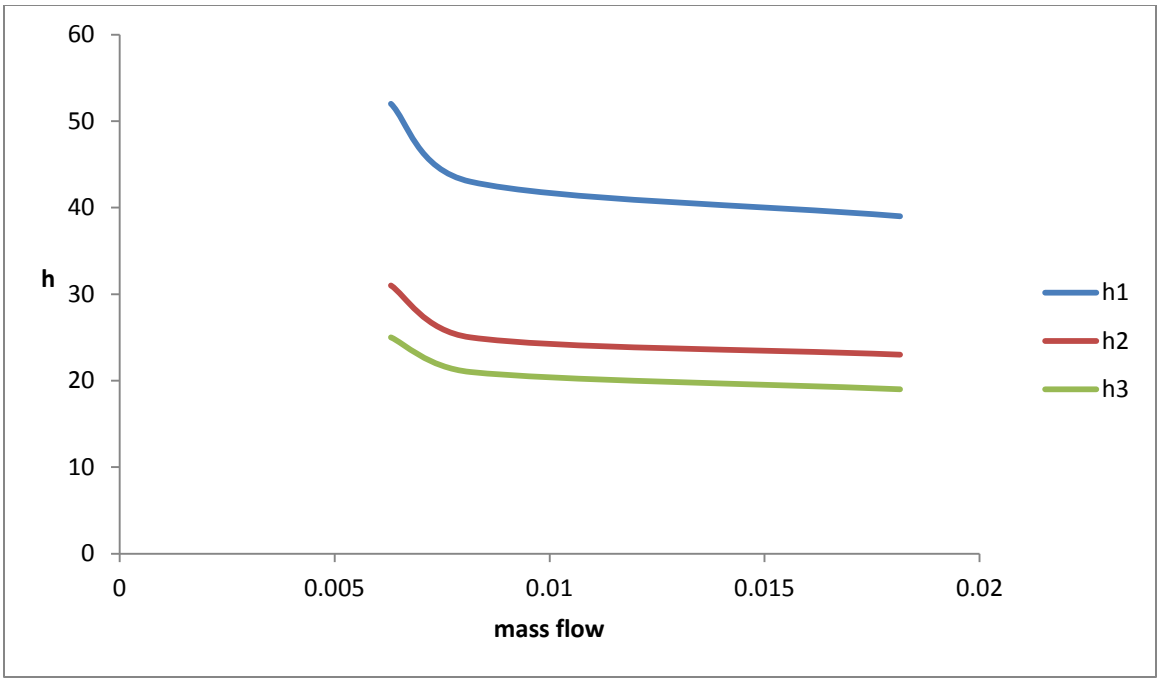

Figure A3: mass flow vs h for 9.52 mm pipe for titanium dioxide.

The data used for development of model and regression analysis used:

Re	**h**	**l**	**k**	**Nu**	**Re**	**Pr**	**dp (nm)**	**dt (mm)**	**dp/dt**	**rp**	**rf**	**rp/rf**
2665.79	24	3	0.5753	125.1521	2665.79	3.8672	30	15.875	1.88976 38E-06	6310	1053	5.992403
	28	3	0.5753	146.0108	2665.79	3.8672	30	15.875	1.88976 38E-06	6310	1053	5.992403
	35	3	0.5753	182.5135	2665.79	3.8672	30	15.875	1.88976 38E-06	6310	1053	5.992403
3079.677	30	3	0.5753	156.4401	3079.677	3.8672	30	12.7	2.36220 47E-06	6310	1053	5.992403

	45	3	0.5753	234.6602	3079.677	3.8672	30	12.7	2.3622047E-06	6310	1053	5.992403
	32	3	0.5753	166.8695	3079.677	3.8672	30	12.7	2.3622047E-06	6310	1053	5.992403
4204.4	45	3	0.5753	234.6602	4204.4	3.8672	30	9.52	3.1512605E-06	6310	1053	5.992403
	49	3	0.5753	255.5189	4204.4	3.8672	30	9.52	3.1512605E-06	6310	1053	5.992403
	62	3	0.5753	323.3096	4204.4	3.8672	30	9.52	3.1512605E-06	6310	1053	5.992403
2112.95	28	3	0.5753	146.0108	2112.95	3.8672	30	9.52	3.1512605E-06	6310	1053	5.992403
	32	3	0.5753	166.8695	2112.95	3.8672	30	9.52	3.1512605E-06	6310	1053	5.992403
	40	3	0.5753	208.5868	2112.95	3.8672	30	9.52	3.1512605E-06	6310	1053	5.992403
2577.23	21	3	0.5725	110.0437	2577.23	4.0062	30	15.875	1.8897638E-06	4230	1032	4.098837
	25	3	0.5725	131.0044	2577.23	4.0062	30	15.875	1.8897638E-06	4230	1032	4.098837
	31	3	0.5725	162.4454	2577.23	4.0062	30	15.875	1.8897638E-06	4230	1032	4.098837
3196.7	29	3	0.57	151.96	3196.7	4.006	30	12.7	2.36220	4230	103	4.098

4			25	51	4	2			47E-06		2	837
	32	3	0.57 25	167.68 56	3196.7 4	4.006 2	30	12.7	2.36220 47E-06	4230	103 2	4.098 837
	35	3	0.57 25	183.40 61	3196.7 4	4.006 2	30	12.7	2.36220 47E-06	4230	103 2	4.098 837
4284.1 1	42	3	0.57 25	220.08 73	4284.1 1	4.006 2	30	9.52	3.15126 05E-06	4230	103 2	4.098 837
	44	3	0.57 25	230.56 77	4284.1 1	4.006 2	30	9.52	3.15126 05E-06	4230	103 2	4.098 837
	54	3	0.57 25	282.96 94	4284.1 1	4.006 2	30	9.52	3.15126 05E-06	4230	103 2	4.098 837
2008.1 5	25	3	0.57 25	131.00 44	2008.1 5	4.006 2	30	9.52	3.15126 05E-06	4230	103 2	4.098 837
	29	3	0.57 25	151.96 51	2008.1 5	4.006 2	30	9.52	3.15126 05E-06	4230	103 2	4.098 837
	37	3	0.57 25	193.88 65	2008.1 5	4.006 2	30	9.52	3.15126 05E-06	4230	103 2	4.098 837
2583.5 8	19	3	0.57 1	99.824 87	2583.5 8	3.96	30	15.8 75	1.88976 38E-06	3890	102 8	3.784 047
	21	3	0.57 1	110.33 27	2583.5 8	3.96	30	15.8 75	1.88976 38E-06	3890	102 8	3.784 047
	25	3	0.57 1	131.34 85	2583.5 8	3.96	30	15.8 75	1.88976 38E-06	3890	102 8	3.784 047

3136.24	23	3	0.571	120.8406	3136.24	3.96	30	12.7	2.3622047E-06	3890	1028	3.784047
	25	3	0.571	131.3485	3136.24	3.96	30	12.7	2.3622047E-06	3890	1028	3.784047
	33	3	0.571	173.38	3136.24	3.96	30	12.7	2.3622047E-06	3890	1028	3.784047
4329.08	39	3	0.571	204.9037	4329.08	3.96	30	9.52	3.1512605E-06	3890	1028	3.784047
	44	3	0.571	231.1734	4329.08	3.96	30	9.52	3.1512605E-06	3890	1028	3.784047
	52	3	0.571	273.2049	4329.08	3.96	30	9.52	3.1512605E-06	3890	1028	3.784047

										0		
1945.17	23	3	0.571	120.8406	1945.17	3.96	30	9.52	3.1512605E-06	3890	1028	3.784047
	25	3	0.571	131.3485	1945.17	3.96	30	9.52	3.1512605E-06	3890	1028	3.784047
	28	3	0.571	147.1103	1945.17	3.96	30	9.52	3.1512605E-06	3890	1028	3.784047

Final table for regression:

Nu	Re	Pr	dp/dt	rp/rf	log Nu	log Re	log Pr	log (dp/dt)	log (rp/rf)
125.1521	2665.79	3.8672	1.89E-06	5.992403	2.097438	3.425826	0.587397	-5.7235925	0.77760099
146.0108	2665.79	3.8672	1.89E-06	5.992403	2.164385	3.425826	0.587397	-5.7235925	0.77760099
182.5135	2665.79	3.8672	1.89E-06	5.992403	2.261295	3.425826	0.587397	-5.7235925	0.77760099
156.4401	3079.677	3.8672	2.36E-06	5.992403	2.194348	3.488505	0.587397	-5.6266825	0.77760099
234.6602	3079.677	3.8672	2.36E-06	5.992403	2.370439	3.488505	0.587397	-5.6266825	0.77760099
166.8695	3079.677	3.8672	2.36E-06	5.992403	2.222377	3.488505	0.587397	-5.6266825	0.77760099
234.6602	4204.4	3.8672	3.15E-06	5.992403	2.370439	3.623704	0.587397	-5.5015157	0.77760099
255.5189	4204.4	3.8672	3.15E-06	5.992403	2.407423	3.623704	0.587397	-5.5015157	0.77760099
323.3096	4204.4	3.8672	3.15E-06	5.992403	2.509619	3.623704	0.587397	-5.5015157	0.77760099
146.0108	2112.95	3.8672	3.15E-06	5.992403	2.164385	3.324889	0.587397	-5.5015157	0.77760099
166.8695	2112.95	3.8672	3.15E-06	5.992403	2.222377	3.324889	0.587397	-5.5015157	0.77760099
208.5868	2112.95	3.8672	3.15E-06	5.992403	2.319287	3.324889	0.587397	-5.5015157	0.77760099
110.0437	2577.23	4.0062	1.89E-06	4.098837	2.041565	3.411153	0.602733	-5.7235925	0.61266067
131.0044	2577.23	4.0062	1.89E-06	4.098837	2.117286	3.411153	0.602733	-5.7235925	0.61266067
162.4454	2577.23	4.0062	1.89E-06	4.098837	2.210707	3.411153	0.602733	-5.7235925	0.61266067
151.9651	3196.74	4.0062	2.36E-06	4.098837	2.181744	3.504707	0.602733	-5.6266825	0.61266067
167.6856	3196.74	4.0062	2.36E-06	4.098837	2.224496	3.504707	0.602733	-5.6266825	0.61266067
183.4061	3196.74	4.0062	2.36E-06	4.098837	2.263414	3.504707	0.602733	-5.6266825	0.61266067
220.0873	4284.11	4.0062	3.15E-06	4.098837	2.342595	3.631861	0.602733	-5.5015157	0.61266067
230.5677	4284.11	4.0062	3.15E-06	4.098837	2.362798	3.631861	0.602733	-5.5015157	0.61266067
282.9694	4284.11	4.0062	3.15E-06	4.098837	2.45174	3.631861	0.602733	-5.5015157	0.61266067
131.0044	2008.15	4.0062	3.15E-06	4.098837	2.117286	3.302796	0.602733	-5.5015157	0.61266067

Pictures of experimental setup:

Ball valve

Temperature sensor

Pipe joint

Insulated part of pipe.

Sensor port.

References

S.S. Mallick, A. Mishra, L. Kundan, An investigation into modelling thermal conductivity for alumina–water nanofluids. Powder Technology 233 (2013) 234–244

Weerapun Duangthongsuk, Somchai Wongwises.Effect of thermo physical properties models on the predicting of the convective heat transfer coefficient for low concentration nanofluid. International Communications in Heat and Mass Transfer 35 (2008) 1320–1326

K.V. Sharma, L. Syam Sundar, P.K. Sharma estimation of heat transfer coefficient and friction factor in the transition flow with low volume concentration of Al_2O_3 nanofluid flowing in a circular tube and with twisted tape insert. International Communications in Heat and Mass Transfer 36 (2009) 503–507

M. Chandra Sekhara Reddy, Veeredhi Vasudeva Rao .Experimental investigation of heat transfer coefficient and friction factor of ethylene glycol water based TiO2 nanofluid in double pipe heat exchanger with and without helical coil inserts. International Communications in Heat and Mass Transfer 50 (2014) 68–76

J. Koo, C. Kleinstreuer, A new thermal conductivity model for nanofluids, Journal

of Nanoparticle Research 6 (2004) 577–588

W.H. Azmi , K.V. Sharma , P.K. Sarma , Rizalman Mamat , Shahrani ,Anuar .Comparison of convective heat transfer coefficient and friction factor of TiO_2 nanofluid flow in a tube with twisted tape inserts. International Journal of Thermal Sciences 81 (2014) 84-93

A. H. Zamzamian, M. Tajik Jamal-Abadi .Factor Effect Estimation in the Convective Heat Transfer Coefficient Enhancement of Al_2O_3/EG Nanofluid in a Double-pipe Heat Exchanger. IJE transactions b: application vol. 26, no. 8, (august 2013) 837-844

W.H.Azmi, K.V.Sharma, Rizalman Mamat, and Shahrani Anuar .Turbulent Forced Convection Heat Transfer of Nanofluids with Twisted Tape Insert in a Circular Tube. International Journal of Thermal Sciences 81 (2014) 84-93

Razvan silviu luciu, Theodor mateescu, Victoria cotoroba and thierry mare, nusselt number and convection heat transfer coefficient for a coaxial heat exchanger using al2o3–water ph=5 nanofluid. Universitatea Tehnic˘a ‚Gheorghe Asachi” din Ias¸I Tomul LV (LIX), Fasc. 2, 2009.

Hyder H. Balla, Shahrir Abdullah, Wan Mahmood Wan Mohd Faizal, Rozli Zulkifli, Kamaruzaman Sopian1 Enhancement of Heat Transfer coefficient Multi-metallic nanofluid with ANFIS Modeling for Thermo physical Properties. http://thermalscience.vinca.rs/online-first/1150

H. Salehi, S. Zeinali-Heris, M. Esfandyari, M. Koolivand. Nero-fuzzy modeling of the convection heat transfer coefficient for the nanofluid. Heat Mass Transfer (2013) 49:575–583

DOI 10.1007/s00231-012-1104-9.

D. V. Guzei, A. V. Minakov, V. Ya. Rudyak, and A. A. Dekterev .Measuring the Heat Transfer Coefficient of Nanofluid Based on Copper Oxide in a Cylindrical Channel. Pis’ma v Zhurnal Tekhnicheskoi Fiziki, 2014, Vol. 40, No. 5, pp. 34–42.

D.P. Kulkarni, P.K. Namburu, H.E. Bargar, D.K. Das, Convective heat transfer and fluid dynamic characteristics of SiO2-ethylene glycol/water nanofluid, Heat Transf. Eng. 29 (12) (2008) 1027-1035.

Y. Ding, H. Alias, D. Wen, R.A. Williams, Heat transfer of aqueous suspensions of Carbon nanotubes (CNT nanofluids), Int. J. Heat Mass Transf. 49 (2006) 240 - 250.

U. Rea, T. McKrell, L.W. Hu, J. Buongiorno, Laminar convective heat transfer and viscous pressure loss of alumina-water and zirconia-water nanofluids, Int. J. Heat Mass Transf. 52 (2009) 2042-2048

Das S.K., Choi S.U.S., Yu W. and Pradeep K., 2007, Nanofluids Science and Technology, Publ.Wiley Interscience

Yoo D.H., Hong K.S. and Yang H.S., 2007, Study of Thermal Conductivity of Nanofluid for The Application of Heat Transfer Fluids', Thermochimic Ata, Vol. 455, PP. 66-69.

Timofeeva E.V., Gavrilov A.N., McCloskey J.M., Tolmachev Y.V., Sprunt S., Lopatina L.M. and Selinger J.V., 2007, Thermal Conductivity and Particle Agglomeration In Alumina Nanofluids: Experiment And Theory, Physical Review E, Vol. 76, Issue. 061703, PP. 1-16.

S.Z. Heris, S.G. Etemad, M.N. Esfahany, Experimental investigation of oxide nanofluids laminar flow convective heat transfer, Int. Commun. Heat Mass Transf. 33 (2006) 529- 535.

M. Hojjat, S. Gh. Etemad, R. Bagheri, J. Thibault, Turbulent forced convection heat transfer of non-Newtonian nanofluids, Exp. Therm Fluid Sci. 35 (2011) 1351–1356

G. Pathipakka, P. Sivashanmugam, Heat transfer behaviour of nanofluids in a uniformly heated circular tube fitted with helical inserts in laminar flow, Superlattices Microstruct. 47 (2010) 349 360

Choi U.S Stephen, Wang H.P., 1995 : Enhancing thermal conductivity of fluids with nanoparticles, Siginer D.A., Developments and Applications of Non-Newtonian Flows, FED-vol. 231/MD-vol. 66, ASME, New York, pp. 99–105.

Yoo D.H., Hong K.S. and Yang H.S., 2007, Study of Thermal Conductivity of Nanofluid for The Application of Heat Transfer Fluids', Thermochimic Ata, Vol. 455, PP. 66-69.

Choi S. U. S., 1999, Nanofluid Technology: Current Status and Future Research, Stephen U.S. Choi Energy Technology Division Argonne National Laboratory Argonne, Il 60439.

Das S.K, Choi S.U.S., W. Yu and K. Pradeep, 2008 : Nanofluids Science and Technology, Wiley Interscience. Applied Physics, 9 131–139.

Akoh H., Tsukasaki Y., Yatsuya S., and Tasaki A., 1978, Magnetic Properties of Ferromagnetic Uhrafine Particles Prepared by a Vacuum Evaporation on Running Oil Substrate, J Cryst. Growth, Vol. 45, PP. 495-500.

Chon C.H., Kihm K.D., Lee S.P. and Choi S.U.S., 2005, Empirical Correlation Finding The Role of Temperature and Particle Size for Nanofluid (Al2O3) Thermal Conductivity Enhancement, Physics Letter, Vol. 87, Issue. 153107, PP. 1-3.

B.C. Pak, Y.I. Cho, Hydrodynamic and heat transfer study of dispersed fluids with submicron metallic oxide particles, Exp. Heat Transf. 11 (1998) 151-170.

Y. Xuan, W. Roetzel, (2000). Conceptions for heat transfer correlation of nanofluids, International Journal of Heat and Mass Transfer, 43 (2000), 3701-3707

S.E.B. Maiga, S.J. Palm, C.T. Nguyen, G. Roy, N. Galanis, Heat transfer enhancement by using nanofluids in forced convection flows. Int. J. Heat Fluid Flow, 26 (2005) 530 - 546.

K.S. Hwang, S.P. Jang, S. U. S. Choi, Flow and convective heat transfer characteristics of Water-based Al_2O_3 nanofluids in fully developed laminar flow regime, Int. J. Heat Mass Transf. 52 (2009) 193-199.

Kwak K. and Kim C., 2005, Viscosity and Thermal Conductivity of Copper Oxide nanofluid .Dispersed In Ethylene Glycol, Korea-Australia Rheology , Vol. 17, Issue. 2, PP. 35-40.

Choi S.U.S., 1995, Developments and Applications of Non-Newtonian Flows, Fed Vol. 231/Md Vol. 66, pp. 99–105.

P.Keblinski, S.R. Phillpot, S.U.S. Choi, J.A. Eastman, Mechanisms of heat flow in suspensions of nano-sized particles (nanofluids), International Journal of Heat and Mass Transfer 45 (2002) 855-863.

M. Rafati, A.A. Hamidi, M. Shariati Niaser. Application of nanofluids in computer cooling systems (heat transfer performance of nanofluids). Applied Thermal Engineering Volumes 45–46, December 2012, Pages 9–14.

G. Donzelli, R. Cerbino, and A. Vailati, "Bistable heat transfer in a nanofluid," Physical Review Letters, vol. 102, no. 10, Article ID 104503, 4 pages, 2009.

S. J. Kim, I. C. Bang, J. Buongiorno, and L. W. Hu, "Study of pool boiling and critical heat flux enhancement in nanofluids," Bulletin of the Polish Academy of Sciences—Technical Sciences, vol. 55, no. 2, pp. 211–216, 2007.

S. J. Kim, I. C. Bang, J. Buongiorno, and L. W. Hu, "Surface wettability change during pool boiling of nanofluids and its effect on critical heat flux," International Journal of Heat and Mass Transfer, vol. 50, no. 19-20, pp. 4105–4116, 2007.

J. Routbort, et al., Argonne National Lab, Michellin North America, St. Gobain Corp.2009,http://www1.eere.energy.gov/industry/nanomanufacturing/pdfs/nanofluids_industrial_cooling.pdf

P. X. Tran, D. K. Lyons, et al., "Nanofluids for Use as Ultra-Deep Drilling Fluids," U.S.D.O.E., 2007, http://www.netl.doe.gov/publications/factsheets/rd/R&D108.pdf.

D. Singh, J. Toutbort, G. Chen, et al., "Heavy vehicle systems optimization merit review and peer evaluation," Annual Report, Argonne National Laboratory, 2006.

M. J. Kao, C. H. Lo, T. T. Tsung, Y. Y. Wu, C. S. Jwo, and H. M. Lin, “Copper-oxide brake nanofluid manufactured using arc-submerged nanoparticle synthesis system,” Journal of Alloys and Compounds, vol. 434-435, pp. 672–674, 2007

Gharagozloo P.E., Goodson K.E., 2010, Aggregate fractal dimensions and thermal conduction in nanofluids, J. Appl. Phys. 108 (7).

Hwang Y., Lee J.K., Lee C.H., Jung Y.M., Cheong S.I., Lee C.G., Ku B.C., Jang S.P., 2007, Stability and thermal conductivity characteristics of nanofluids, Thermochimic Acta 455, 70-74.

Keblinski P., Prasher R., Eapen J., 2008, Thermal Conductance of nanofluids: is the controversy over?, J Nanopart RES 10: 1089-1097.

Hong K.S., Hong T.K., 2006, Thermal conductivity of Fe nanofluids depending on the cluster size of nanoparticles, Appl. Phys. Lett. 88 (3) 1-3.